Contrib Mineral Petrol (2000) 138: 127–142

A. Kröner · P.J. O'Brien · A.A. Nemchin · R.T. Pidgeon

Zircon ages for high pressure granulites from South Bohemia, Czech Republic, and their connection to Carboniferous high temperature processes

Received: 25 February 1999 / Accepted: 27 September 1999

Abstract Petrological and isotopic investigations were undertaken on high pressure granulites of granitic to mafic composition from the Prachatice and Blanský les granulite complexes of southern Bohemia, Czech Republic. The predominant felsic granulites are quartz + ternary feldspar (now mesoperthite)-rich rocks containing minor garnet, kyanite and rutile, and most show a characteristic mylonitic fabric formed during retrogression along the exhumation path. Three high temperature reaction stages at distinctly different pressures are recognized. Rare layers of intermediate to mafic composition, containing clinopyroxene, best record a primary high pressure–high temperature stage (>15 kbar, >900 °C), and a well-defined overprint at medium pressure granulite facies conditions (6–8 kbar, 700–800 °C) during which orthopyroxene (+plagioclase) formed from garnet and clinopyroxene. A further high temperature overprint at lower pressure (ca. 4 kbar) is reflected in the development of cordierite- and/or andalusite-bearing partial-melt patches in some felsic granulites.

Conventionally separated zircons from the granulites were measured on a SHRIMP II ion microprobe. Near-spherical, multifaceted grains interpreted to be metamorphic, and short prismatic grains from the cordierite-bearing melt patch, are all concordant and yielded indistinguishable results producing an average age, for 83 individual grain spots, of 339.8 ± 2.6 Ma (2σ). Metamorphic grains from a meta-granodiorite associated with the granulites gave the same age (339.6 ± 3.1 Ma, mean of 9), whereas inherited magmatic grains of the same sample yielded 367.8 ± 1.4 Ma. A mean age of 469.3 ± 3.8 Ma was obtained for two short prismatic concordant grains in one of the granulites, whereas several of the rounded grains with ca. 340 Ma metamorphic zircon overgrowths had much older ($^{207}Pb/^{206}Pb$ minimum ages up to 1771 Ma) discordant cores. In addition to analysis of conventionally separated grains, ion-microprobe measurements were also made on zircons extracted from thin sections (drilled-out, mounted and repolished) such that a direct relationship between the dated zircons and petrographic position could be made. Identical results were obtained from both preparation methods, thus showing that the considerable advantage in petrological control is not offset by any appreciable lack of precision when compared to conventionally prepared ion-microprobe samples. All these isotopic results are identical to those previously obtained by conventional multigrain and single-grain evaporation techniques, but rather than allowing a greater resolution of the age of the petrographically obvious different metamorphic stages the results document, for the first time, the apparent short time scale for high, medium and low pressure metamorphism in the granulites. The short time period between the 340 Ma age for the high pressure granulites, as derived here and from studies of similar rocks elsewhere in the European Variscides, and the 320–330 Ma ages for regional low pressure–high temperature metamorphism, migmatization and granite magmatism, strongly suggests an important link between these two high temperature processes.

A. Kröner (✉)
Institut für Geowissenschaften, Universität Mainz,
55099 Mainz, Germany
e-mail: kroener@mail.uni-mainz.de
Tel.: +49-6131-3922163; Fax: +49-6131-3924769

P.J. O'Brien
Bayerisches Geoinstitut, Universität Bayreuth,
Postfach 101251, 95440 Bayreuth, Germany

A.A. Nemchin · R.T. Pidgeon
Department of Applied Geology,
Curtin University of Technology, Bentley, 6012 WA, Australia

Editorial responsibility: W. Schreyer

Introduction

Granulite facies rocks are important in the reconstruction and evaluation of orogenic processes as they represent crustal material transformed at the highest grade (i.e. temperature) of metamorphism at conditions where melting (i.e. magmatic) processes are prevalent. These conditions can be those of a stable lower crustal geotherm or, alternatively, those attained during the peak of regional metamorphism. Many of the large, exposed granulite domains around the world were formed in the Precambrian, but most were exhumed by much later tectonism and so yield long-term information pertaining to conditions and processes in the lower continental crust.

The most voluminous of the scattered granulite relics in the crystalline core of the European Variscides are high pressure (HP), kyanite–K-feldspar-bearing varieties of granitic composition (e.g. Pin and Vielzeuf 1983; Fiala et al. 1987). Although a Precambrian age was proposed for a certain number of these (e.g. Neumann 1984), all geochronological studies have produced Palaeozoic, and in many cases Carboniferous, ages for the metamorphism (van Breemen et al. 1982; Schenk and Todt 1983; Aftalion et al. 1989; von Quadt 1993; Wendt et al. 1994; Kröner et al. 1995; Kotková et al. 1996; Becker 1997; O'Brien et al. 1997a; Kröner and Willner 1998). The implied short time scale for formation and exhumation means that this type of granulite is important as a source of information on orogenic processes. An understanding of the formation, exhumation, (partial) modification and (partial) preservation of the granulites will provide important information for the interpretation of the Palaeozoic, and especially Variscan, evolution of the European basement. The purpose of the present study is to investigate the cause of extremely high crustal temperatures and widespread magmatism at both deep (>15 kbar) and shallow (<5 kbar) crustal levels during the Palaeozoic evolution of the southern Bohemian Massif. To accomplish this we have determined the U–Pb ages of zircon generations at petrologically identifiable temperature points in the metamorphic evolution.

Our method was to make detailed ion-microprobe investigations of single zircons, either handpicked from heavy mineral concentrates, or extracted directly from thin sections by means of a micro-drill and remounting the zircons for SHRIMP analysis. The great advantage of the latter technique is that there is direct petrographic control on the zircons selected for isotopic measurement. What we have been designating as metamorphic zircons are near-spherical, multifaceted ("football-shaped") predominantly transparent grains with high reflectivity. The morphologically distinct grains can easily be distinguished from detrital grains that have round and "pitted" surfaces. Many such metamorphic zircons have been documented from granulite facies terrains in central Europe by Hoppe (1962), and their formation during high-grade metamorphism was proposed by Pidgeon and Bowes (1972), who dated such grains from the Lewisian of Scotland. In recent years, several geochronological studies of metamorphic zircons (Kröner et al. 1994, 1998; Kotková et al. 1996; Jaeckel et al. 1997; O'Brien et al. 1997a; Kröner and Willner 1998) produced precise ages that were interpreted to reflect the peak of granulite facies metamorphism (Kröner and Jaeckel 1995).

The particular problems addressed in this study were: (1) the age of zircon formation; (2) whether zircon growth was in a magmatic or a metamorphic environment; (3) the degree of any modification of zircon (and constituent isotopes) such as by overgrowth, dissolution or diffusion; and (4) the relationship between the zircon history and that reflected by the petrological evolution identifiable from major mineral constituents.

Geological setting

The largest concentration of granulite bodies in central Europe (Fig. 1) occurs in southern Bohemia, Czech Republic (Fiala et al. 1987; Fiala 1995), close to the town of Česke Budějovice (better known by beer-lovers under the name of Budweis). The largest bodies are the Blanský les (25×15 km), Křištanov, Prachatice and Lišov massifs, although much smaller bodies are strewn along a NE–SW-trending belt for almost 100 km. The south Bohemian granulite bodies, like their counterparts in neighbouring Lower Austria, comprise part of the Gföhl Unit, the tectonically uppermost of a series of nappe units forming the high grade Moldanubian Zone of the southern Bohemian Massif (Fuchs 1971, 1991, 1995; Fiala 1995). Apart from the granulites, which enclose bodies

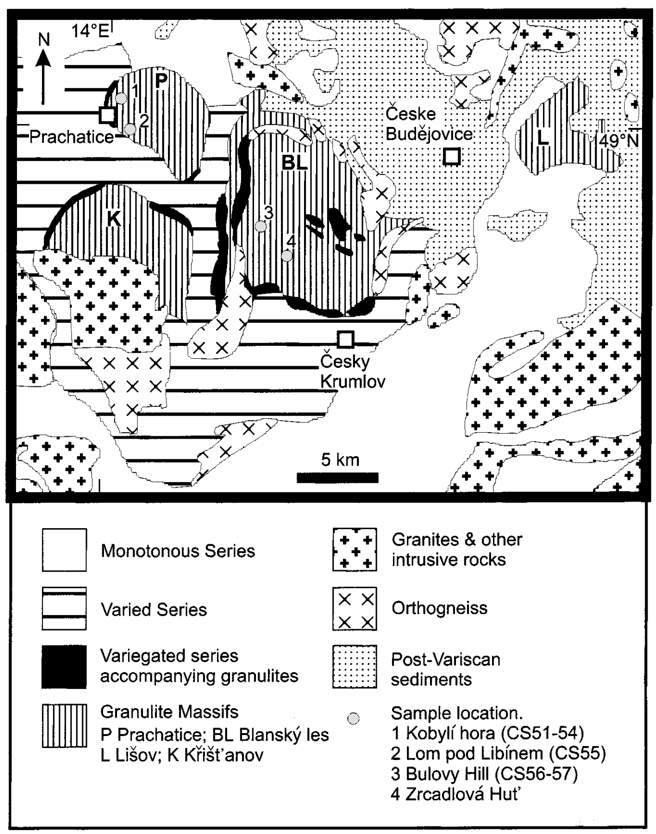

Fig. 1 Simplified and schematic geological map of the granulite massifs in South Bohemia showing major rock units and location of samples dated in this study

of serpentinized garnet peridotite, pyroxenites and sometimes also high-temperature eclogites, the composite Gföhl Unit also contains a polydeformed, migmatitic, granitic gneiss (Gföhl gneiss, probably overprinted granulite) and variegated, amphibolite-rich units structurally below the granulites (Fuchs 1995). Successively underlying the granulite-bearing unit, and areally more extensive, are the Varied and Monotonous Series (Zoubek 1974). Gneisses enclosing abundant alternations of orthogneisses, amphibolites, marbles, calc-silicate rocks, metaquartzites and graphitic schists in the aptly named Varied Series contrast with uniform paragneisses in the Monotonous Series containing only localized meta-eclogite (O'Brien and Vrána 1995; O'Brien et al. 1997b). Microfossils have been interpreted as indicating a Palaeozoic protolith age for some paragneisses (Konzalov 1980; Pacltov 1994), whereas some orthogneisses from both the Austrian (1.38 Ga; Gebauer and Friedl 1994) and Czech parts (2.1 Ga; Wendt et al. 1993), grouped with the Varied Series, have yielded Precambrian protolith ages. Syn- to post-orogenic granites dated at 300–330 Ma (Friedl et al. 1993) and $^{40}Ar/^{39}Ar$ cooling ages clustering around 330 Ma from micas and amphiboles of Varied Series metamorphic rocks (Dallmeyer et al. 1992) mark the end of the orogeny.

Previous geochronological studies of the granulites and related rocks from southern Bohemia have yielded a range of ages and a range of interpretations. Conventional multigrain zircon size and/or magnetic fraction U–Pb measurements, ion-microprobe (SHRIMP) spot analysis undertaken without the benefit of cathodoluminescence study, and investigations by the evaporation method, all indicated the presence of old (early Proterozoic to Archaean) components and either partial resetting or new components (overgrowths) as the result of Carboniferous metamorphism around 340 Ma (van Breemen et al. 1982; Aftalion et al. 1989; Wendt et al. 1994; Kröner et al. 1998). Monazite U–Pb data from various parts of the Gföhl Unit are either concordant or plot on well-defined discordia lines intersecting concordia at 340 Ma (van Breemen et al. 1982; Schenk and Todt 1983; Friedl et al. 1994). The 340 Ma age, and a second cluster of results around 370 Ma, have also been deduced by Sm–Nd dating of granulites as well as garnet pyroxenite and eclogite from peridotite bodies within both the Czech and Austrian parts of the Gföhl Unit (Carswell and Jamtveit 1990; Brueckner et al. 1991; Beard et al. 1992; Medaris et al. 1995; Becker 1997). The Carboniferous age for metamorphism in the Gföhl Unit from zircon and monazite dating contrasts considerably with the results from Rb–Sr whole-rock investigations which yielded early Palaeozoic isochron and errochron ages (Arnold and Scharbert 1973; van Breemen et al. 1982; Frank et al. 1990).

General sample description, petrography and mineral chemistry

The investigated samples come from the Blanský les and Prachatice complexes (Fig. 1) within which the dominant rock type is pyroxene-free, quartz + K-feldspar-rich felsic granulite, of granitic composition, containing garnet, kyanite and rutile. Pyroxene-bearing granulites of intermediate to mafic composition, along with ultramafic rocks (serpentinized garnet peridotites and pyroxenites), comprise less than 20% of the complexes (Fiala et al. 1987). An intense flattening fabric (D_3 of Vrána 1979), which locally produced blastomylonites, is intimately linked to an increase in biotite and sillimanite content, i.e. a retrograde assemblage. For this reason we deliberately selected biotite-poor rocks with a less distinct foliation as these preserve most relics of the early metamorphic stages. Single zircon U–Pb ion-microprobe studies were undertaken on samples chosen from the Kobylí hora (samples CS 51–54) and Lom pod Libínem (CS 55) quarries in the Prachatice massif and from Bulovy Hill (CS 56–57) at the western edge of the Blanský les massif (Fig. 1). In addition, granulites were collected from the Zrcadlová Hut quarry (Blanský les) for petrologic study. Samples from the Zrcadlová Hut location have already featured in the dating studies of van Breemen et al. (1982) and Wendt et al. (1994), but for the present work a rock of more mafic composition was chosen from here (CB 1.4c). This is because, in contrast to the felsic granulites that form the majority of the investigated material, such clinopyroxene-bearing granulites have proven to be the most reliable for elucidating the metamorphic evolution of the granulite massifs (e.g. Carswell and O'Brien 1993; O'Brien et al. 1997a).

Granulite of mafic composition

The sample from the Zrcadlová Hut quarry contains garnet, clinopyroxene, orthopyroxene, plagioclase, antiperthite, hornblende, quartz, rutile, titanite, ilmenite, apatite and zircon. Rounded anhedral *garnet*, up to 1.5 mm but mostly less than 0.75 mm across, is compositionally zoned with X_{Mg} [Mg/(Mg + Fe)] lower at the rim than in the core (e.g. core: $X_{Alm} = 0.44$, $X_{Prp} = 0.31$, $X_{Grs} = 0.23$, $X_{Sps} = 0.02$, $X_{Mg} = 0.42$; rim; $X_{Alm} = 0.616$, $X_{Prp} = 0.167$, $X_{Grs} = 0.17$, $X_{Sps} = 0.047$, $X_{Mg} = 0.21$). Smaller grains have higher core X_{Mg} (but lower Ca), whereas peak X_{Mg} in larger grains occurs between core and rim but at constant Ca. Inclusions, generally few and small, are rutile, quartz, apatite, zircon and ilmenite. In places garnet forms incomplete coronas, sometime with perfectly straight crystal faces, around large plagioclase or antiperthite crystals.

Clinopyroxene, larger than garnet (mostly 0.5–3 mm) and typically poikiloblastic or skeletal, encloses large inclusions of plagioclase, antiperthite, quartz and rare garnet (now replaced) as well as some grains of apparently primary biotite. Compositionally, the clinopyroxene corresponds to diopside and, although less strongly zoned than garnet, shows a variation in X_{Mg} from interior ($Ca_{0.86}Na_{0.04}Fe_{0.29}Mg_{0.69}Al^{VI}{}_{0.09}Si_{1.95}Al^{IV}{}_{0.06}O_6$, $X_{Mg} = 0.7004$) towards rims ($Ca_{0.86}Na_{0.02}Fe_{0.37}Mg_{0.67}$ $Al^{VI}{}_{0.04}Si_{1.97}Al^{IV}{}_{0.05}O_6$, $X_{Mg} = 0.644$) as well as irregularly shaped domains with lower Al where topotactic replacement by amphibole (edenite) has occurred. Further varieties of clinopyroxene occurring in a symplectitic intergrowth with ilmenite and as tiny idiomorphic inclusions in antiperthite have lower Al (around 1 wt% Al_2O_3) than the poikiloblast cores.

Brown matrix *amphibole* grains, up to 2 mm in size, enclose plagioclase, antiperthite, clinopyroxene, large biotite grains, apatite and minor rutile, and are in places rimmed by orthopyroxene.

The *orthopyroxene* in this sample appears as coronas around clinopyroxene, quartz close to garnet, or amphibole and in radiating kelyphites replacing garnet, and thus clearly does not belong to the primary assemblage. As is typical for these textural forms, orthopyroxene in the kelyphite has a slightly higher Al content and is more magnesian (~1.4 wt% Al_2O_3 and $X_{Mg} = 0.54$) than the coronitic varieties (~0.75 wt% Al_2O_3 and $X_{Mg} = 0.5$).

Feldspars, an important constituent of the rock, are found in both primary and secondary textures. Matrix plagioclase (An_{30}), although zoned to more Ca-rich rims, is less calcic than that appearing as inclusions in clinopyroxene (~An_{43}), in corona textures with orthopyroxene (~An_{54}) or in the kelyphites around garnet (up to An_{90}). Plagioclase of the antiperthite, like the matrix grains, has an An content around 30 mol% (Or $<$ 4%), whereas the exsolved K-feldspar contains negligible Ca and only around 3 mol% albite.

A few *titanite* grains up to 0.3 mm in size are present in the matrix, but more common titanite has been partially or totally replaced by a symplectitic intergrowth, up to 1 mm in length, of ilmenite and clinopyroxene. Other minor phases are rutile, apatite, zircon and sulphides.

Felsic granulites

Typical for the studied felsic granulites, an indistinctly foliated, light-coloured rock dotted with small ($<$0.5 mm) pink garnets, is the greater part of sample CS 55 from the quarry at Kobylí hora (Fig. 1). The hand specimen is crossed by a 6-cm-wide band containing significantly more abundant, and larger (dominantly 1 mm), garnets and dark biotite grains aligned parallel to the direction of the banding. Quartz and antiperthite dominate in the garnet-poor part and enclose small (generally 0.2–0.4 mm) garnets, kyanite, and minor trains of small (0.05–0.2 mm) grains of biotite defining the foliation. Accessory phases are spinel, apatite, zircon, rutile (often as very long needles) and ilmenite. The largest grains are elongate quartz crystals (up to 2 mm long), whereas most of the feldspar occurs in irregularly shaped subgrains or has recrystallized to a granoblastic two-feldspar (plagioclase $X_{An} = 0.35$–0.4 and perthitic K-feldspar) texture. In the garnet-rich zone the quartz–feldspar texture is the same as in the garnet-poor part although larger (up to 2 mm) antiperthite grains are often present (reconstituted composition $X_{An} = 0.207$, $X_{Ab} = 0.406$, $X_{Or} = 0.386$). More abundant in this part of the sample, and commonly restricted to the edge of garnet which it is clearly replacing, is biotite ($X_{Mg} = 0.6$–0.64, TiO_2 ~5 wt%). Rare kyanite relics in both domains show a partial breakdown to spinel ($X_{Mg} = 0.36$) $\pm$ corundum, set in a more calcic plagioclase (An_{40}), and provide an important guide to a second garnet generation. Locally kyanite has partially (or totally) transformed to sillimanite, but discrete planar zones of secondary sillimanite also occur. The texturally early garnet, generally in contact with matrix antiperthite grains, is larger, poikiloblastic to skeletal in form, and commonly encloses large inclusions of antiperthite and quartz (along with minor apatite, zircon, rutile and rarely kyanite). This contrasts with the second generation of garnet that commonly encloses spinel and/or ilmenite (although plagioclase and corundum are also not uncommon) in the form of chains, aggregates and coronas set within moats of granoblastic plagioclase (An_{40}: the most calcic of the samples). Early garnet (core: $X_{Alm} = 0.57$, $X_{Prp} = 0.32$, $X_{Grs} = 0.10$, $X_{Sps} = 0.01$, $X_{Mg} = 0.36$) shows a sharp fall in Ca towards feldspar, but X_{Mg} at rims is strongly a product of proximity to secondary biotite. The same grain can have rim compositions of $X_{Alm} = 0.6$, $X_{Prp} = 0.36$, $X_{Grs} = 0.03$, $X_{Sps} = 0.01$, $X_{Mg} = 0.375$ towards (but not necessarily in contact to) biotite and $X_{Alm} = 0.65$, $X_{Prp} = 0.3$, $X_{Grs} = 0.03$, $X_{Sps} = 0.01$, $X_{Mg} = 0.31$ on the side away from biotite. This lack of a concentric X_{Mg} distribution in garnet strongly suggests slow grain boundary diffusion due to the absence of a pervasive fluid phase in the rock (O'Brien 1999). The second garnet generation contains small spots representing early nuclei within the Ca-rich plagioclase of the kyanite breakdown domain that are even more Ca-rich than the interiors of the first-formed garnet ($X_{Alm} = 0.6$, $X_{Prp} = 0.23$, $X_{Grs} = 0.15$, $X_{Sps} = 0.02$) but with a significantly lower X_{Mg} of 0.275 (as for the rims of the same grains: $X_{Alm} = 0.67$, $X_{Prp} = 0.28$, $X_{Grs} = 0.03$, $X_{Sps} = 0.02$, $X_{Mg} = 0.3$).

In some cases, as in felsic granulite sample CS 52 (also from Kobylí hora), late cordierite has formed at the expense of biotite and sillimanite. Locally, the cordierite mimics the biotite–sillimanite fabric, but it also forms in small melt pockets that cross-cut the domain fabric.

Geothermobarometry in the granulites

The clear reaction textures and compositional variation or zoning in garnet and feldspar makes accurate geothermobarometry in these rocks problematic. Nevertheless, it is clear that clinopyroxene was present before orthopyroxene in the mafic granulite and that early garnet in the felsic granulites formed in a paragenesis with ternary feldspar, kyanite and quartz. Textural evidence – garnet coronas on idiomorphic feldspar or skeletal garnets with large antiperthite inclusions – suggests a high-pressure melt origin for these rocks (Vrána and Jakeš 1982; Vrána 1989; Carswell and O'Brien 1993; Kotková and Harley 1997). Minimum temperatures for the formation of the ternary feldspar (reconstituted composition) in the felsic granulite, by two-feldspar geothermometry (Fuhrman and Lindsley 1988), lie above 1000 °C for pressures between 10 and 20 kbar. Taking the anorthite activity of the same reconstituted ternary feldspar and the Ca-component of the core of the first-formed garnet yields pressures around 18 kbar (Koziol and Newton 1989: GASP geobarometry). Geothermometry with secondary biotite ($X_{Mg} = 0.6$–0.64) and adjacent garnet rims indicates 750–850 °C with the Fe–Mg exchange thermometer of Ferry and Spear (1978). Utilizing garnet core analyses would result in values up to 150 °C higher, but garnet cores clearly belong to an earlier metamorphic stage. Spinel growth is common around kyanite relics (and sillimanite after kyanite), but the formation conditions are difficult to constrain. If part of the primary garnet rim not affected by biotite is taken to be the composition in equilibrium with spinel (note how similar its composition is to the majority of the second garnet) then conditions around 3–4 kbar (for temperatures of around 700 °C) can be deduced, i.e. in the sillimanite field. The growth of cordierite in discordant melt patches would also be consistent with these conditions as often determined in the more widespread paragneisses of the surrounding Moldanubian Monotonous Series (e.g. Linner 1996).

Geothermobarometry in the mafic granulite sample with the initial garnet(core)–clinopyroxene(core)–matrix plagioclase(core)–quartz assemblage, using the multi-equilibrium program TWEEQU (Berman 1991) (activity models: garnet, Berman 1990; feldspar, Fuhrman and Lindsley 1988; pyroxene, ideal mixing on sites), results in similar high-pressure–high-temperature conditions around 970–1000 °C, 16–17 kbar. These conditions are substantially different to those estimated for the orthopyroxene-bearing assemblage (orthopyroxene and plagioclase along with garnet rim and quartz) which cluster around 700 °C, 6 kbar for corona-type orthopyroxene and at temperatures down to 600 °C for the fine-grained kelyphite orthopyroxene (that has undoubtedly been reset to lower X_{Mg} during cooling). Reactions relating to the ilmenite + clinopyroxene growth from titanite (+garnet) yield a maximum pressure (i.e. titanite no longer stable) of 8 kbar at the same temperature, whereas two-pyroxene geothermometry with compositions from the corona orthopyroxene and the immediately adjacent clinopyroxene rim yields ca. 730 °C (Brey and Köhler 1990) in the same pressure range.

Sample preparation and SHRIMP analytical procedures

Heavy minerals were separated from whole-rock samples CS 51–57 by standard procedures using jaw crusher, steel rolling mill, Franz magnetic separator and heavy liquids. Zircons were then hand-picked and mounted in epoxy resin together with chips of the Perth Consortium standard CZ3. The mount was then polished and zircons were photographed in reflected and transmitted light to enable easy location on the mount during SHRIMP analyses. The mount was then cleaned and gold-coated.

In order to check that there was no sampling bias from the normal crush-separate-pick preparation we have successfully tested a new technique. Here, zircons were identified in polished thin sections whereby it was possible to define exactly the relationship to the minerals belonging to the different metamorphic stages. As these were normal microprobe sections it was also simple to evaluate the zircons by cathodoluminescence before selection for isotopic analysis. The parts of the section containing the selected zircons were cut out at the Geoinstitut in Bayreuth, using a microscope-mounted drilling device (Medenbach Company, Bochum). These tiny (200–500 μm diameter) extracted rock slices were then remounted, along with small slivers of the CZ3 zircon standard, and repolished ready for gold-coating and ion-microprobe measurement. The great advantage of this technique is that we have very good petrological control of the zircon location as well as having a sample that conforms to the tight constraints demanded by the ion microprobe. A normal thin section is likely to have only a few widely scattered zircons that would be difficult to locate during measurement and that would require frequent sample changing. Also, it is not easy to mount and polish the necessary pieces of standard zircon within an existing thin section.

Isotopic analyses were performed on the Perth Consortium SHRIMP II ion microprobe whose instrumental characteristics were described by Kennedy and De Laeter (1994). The analytical procedures are outlined in Compston et al. (1992), Claoué-Long et al. (1995) and Nelson (1997). Prior to each analysis, the surface of the analysis site was precleaned by rastering of the primary beam for 2 min, to reduce the surface common Pb. The reduced $^{206}Pb/^{235}U$ ratios were normalized to 0.09432, which is equivalent to an age of 564 Ma. Pb/U ratios in the unknown samples were corrected using the ln(Pb/U)/ln(UO/U) relationship as measured in standard CZ3 and as outlined in Compston et al. (1984) and Nelson (1997). The 1−σ error in the ratio $^{206}Pb/^{238}U$ during analysis of all standard zircons during this study was between 1.20 and 1.48%. Primary beam intensity was between 2.2 and 3.8 nA, and a Köhler aperture of 100 μm diameter was used, giving a slightly elliptical spot size of about 30 μm. Peak resolution was about 4900, enabling clear separation of the ^{208}Pb-peak from the HfO peak. Sensitivity varied between 19 and 36 cps/ppm Pb. Analyses of samples and standards were alternated to allow assessment of Pb^+/U^+ discrimination.

Raw data reduction and error assessment followed the method described by Nelson (1997). Common Pb corrections have been applied using the ^{204}Pb-correction method and assuming the isotopic composition of Broken Hill, since common Pb is thought to be surface-related (Kinny 1986). The analytical data are presented in Table 1. Errors given on individual analyses are based on counting statistics and are at the 1−σ level and include the uncertainty of the standard added in quadrature. Errors for pooled analyses are at 2−σ or 95% confidence.

The $^{207}Pb/^{206}Pb$ SHRIMP ages reported in Table 1 are quite imprecise since the ion microprobe is not suited for accurate measurement of $^{207}Pb/^{206}Pb$ ages of young zircons that have low uranium contents. Small differences in radiogenic $^{207}Pb/^{206}Pb$ imply large differences in apparent age, and the uncertainties in measuring small amounts of radiogenic ^{207}Pb due to low count rates and the sensitivity to the common Pb correction combine to make the corrected $^{207}Pb/^{206}Pb$ relatively imprecise. On the other hand, the $^{206}Pb/^{238}U$ ratio can be determined to a precision of 2–3% on SHRIMP, and if the effects of post-crystallization Pb loss are negligible and no inherited radiogenic Pb is present, the resulting $^{206}Pb/^{238}U$ age provides the most accurate estimate of the age for the grain domain analysed (Williams and Claesson 1987).

Zircon cathodoluminescence and backscattered electron imagery

Zircons from both the epoxy and thin section mounts were examined under cathodoluminescence and backscattering imagery using a JEOL JXA-8900RL microprobe at the University of Mainz. Operating conditions were 15 kV accelerating voltage and 12 nA beam current.

Hanchar and Miller (1993) have summarized the principles of cathodoluminescence (CL) and backscattered electron (BSE) imagery and its usefulness to elucidate the internal structure, zonation and growth history of zircons. While CL spectra are primarily controlled by trace constituents in zircon, particularly the REE, BSE reveals contrasts in average atomic number of regions of a mineral phase, i.e. the higher the number the brighter the area (e.g. Paterson et al. 1989). CL and

Table 1 SHRIMP II analytical data for spot analyses of single zircons from South Bohemian granulites, Czech Republic

Sample no.[a]	U (ppm)	Th (ppm)	$^{206}Pb/^{204}Pb$	$^{208}Pb/^{206}Pb$	$^{207}Pb/^{206}Pb$	$^{206}Pb/^{238}U$	$^{207}Pb/^{235}U$	206/238 age ± 1σ	207/235 age ± 1σ	207/206 age ± 1σ
CS 51r-1-1	518	177	2182	0.1077 ± 29	0.0560 ± 12	0.0709 ± 10	0.547 ± 15	441 ± 6	443 ± 10	453 ± 48
CS 51r-1-2	250	43	6964	0.0526 ± 38	0.0530 ± 17	0.0545 ± 8	0.399 ± 15	342 ± 5	340 ± 11	328 ± 75
CS 51r-2-1	827	1865	2271	0.7073 ± 37	0.0538 ± 11	0.0576 ± 8	0.427 ± 11	361 ± 5	361 ± 8	361 ± 47
CS 51r-2-2	248	39	4559	0.0463 ± 28	0.0526 ± 14	0.0544 ± 8	0.395 ± 12	341 ± 5	338 ± 9	313 ± 61
CS 51r-3-1	359	42	4159	0.0353 ± 25	0.0540 ± 11	0.0638 ± 9	0.475 ± 13	399 ± 6	395 ± 9	373 ± 48
CS 51r-3-2	246	42	182282	0.0534 ± 12	0.0540 ± 8	0.0547 ± 8	0.400 ± 9	344 ± 5	342 ± 7	331 ± 37
CS 51r-4-1	866	1586	6271	0.5747 ± 27	0.0538 ± 6	0.0571 ± 8	0.424 ± 8	358 ± 5	359 ± 6	362 ± 29
CS 51r-4-2	382	46	1328	0.0364 ± 45	0.0530 ± 19	0.0541 ± 7	0.395 ± 16	340 ± 5	338 ± 12	328 ± 83
CS 51r-5	128	65	7784	0.1613 ± 47	0.0535 ± 20	0.0542 ± 6	0.400 ± 16	340 ± 4	341 ± 12	349 ± 83
CS 51r-6	136	42	6474	0.0942 ± 69	0.0531 ± 30	0.0546 ± 6	0.400 ± 24	342 ± 4	341 ± 17	427 ± 41
CS 51r-7	256	40	1000	0.0516 ± 69	0.0537 ± 30	0.0541 ± 7	0.400 ± 23	339 ± 5	342 ± 17	357 ± 122
CS 51r-8	204	53	436	0.0805 ± 110	0.0529 ± 47	0.0541 ± 8	0.395 ± 36	340 ± 5	338 ± 26	326 ± 191
CS 51l-9	676	58	4907	0.0275 ± 22	0.0546 ± 10	0.0653 ± 9	0.492 ± 12	408 ± 6	406 ± 8	397 ± 41
CS 51l-10	499	78	1916	0.0494 ± 29	0.0534 ± 13	0.0571 ± 8	0.421 ± 12	358 ± 5	356 ± 9	345 ± 54
CS 51l-11	292	32	1153	0.0360 ± 55	0.0538 ± 24	0.0568 ± 8	0.421 ± 21	356 ± 5	357 ± 15	362 ± 102
CS 52p-1-1	386	620	827	0.5024 ± 58	0.0551 ± 21	0.0674 ± 9	0.512 ± 22	421 ± 6	420 ± 15	415 ± 85
CS 52p-1-2	117	69	1972	0.1877 ± 72	0.0536 ± 30	0.0545 ± 8	0.403 ± 24	342 ± 5	344 ± 18	357 ± 124
CS 52r-3-1	420	123	798	0.0902 ± 54	0.0528 ± 23	0.0540 ± 7	0.393 ± 18	339 ± 5	337 ± 14	318 ± 97
CS 52r-3-2	193	68	2544	0.1070 ± 48	0.0518 ± 21	0.0544 ± 8	0.389 ± 17	341 ± 5	333 ± 13	277 ± 91
CS 52p-4-1	198	73	3915	0.1131 ± 80	0.0531 ± 35	0.0540 ± 6	0.395 ± 27	339 ± 4	338 ± 20	332 ± 144
CS 52r-4-2	209	70	5781	0.1080 ± 34	0.0538 ± 15	0.0548 ± 8	0.407 ± 14	344 ± 5	347 ± 10	364 ± 65
CS 52p-5-1	185	137	3453	0.2308 ± 56	0.0530 ± 22	0.0540 ± 6	0.394 ± 18	339 ± 4	338 ± 13	329 ± 95
CS 52r-5-2	174	65	2483	0.1222 ± 7	0.0553 ± 36	0.0543 ± 8	0.414 ± 26	341 ± 5	352 ± 19	423 ± 130
CS 52r-6-1	399	169	4385	0.1330 ± 26	0.0536 ± 11	0.0541 ± 6	0.400 ± 10	340 ± 4	341 ± 7	355 ± 47
CS 52r-6-2	169	57	8355	0.1045 ± 40	0.0527 ± 18	0.0547 ± 8	0.398 ± 15	344 ± 5	340 ± 11	317 ± 77
CS 52r-7	424	137	8369	0.1015 ± 23	0.0531 ± 11	0.0542 ± 6	0.397 ± 10	340 ± 4	339 ± 7	335 ± 46
CS 52r-8	269	57	8981	0.0666 ± 20	0.0533 ± 10	0.0474 ± 5	0.348 ± 8	299 ± 4	303 ± 6	340 ± 44
CS 52r-9-1	261	70	3251	0.0821 ± 79	0.0527 ± 34	0.0541 ± 6	0.393 ± 27	339 ± 4	336 ± 20	316 ± 144
CS 52r-9-2	162	73	1950	0.1279 ± 48	0.0545 ± 20	0.0544 ± 7	0.409 ± 16	342 ± 5	348 ± 12	390 ± 81
CS 52r-10	35	30	221	0.2524 ± 434	0.0585 ± 184	0.0553 ± 12	0.446 ± 142	347 ± 8	374 ± 95	547 ± 571
CS 52r-11	339	81	1705	0.0663 ± 42	0.0526 ± 18	0.0541 ± 7	0.392 ± 15	340 ± 5	336 ± 11	310 ± 78
CS 52r-12	93	50	628	0.1514 ± 110	0.0547 ± 46	0.0541 ± 7	0.408 ± 35	339 ± 5	307 ± 25	401 ± 178
CS 52r-13	308	61	3112	0.0781 ± 29	0.0683 ± 13	0.0764 ± 10	0.720 ± 18	475 ± 6	551 ± 10	879 ± 39
CS 52r-14	673	90	1109	0.0430 ± 48	0.0535 ± 21	0.0539 ± 7	0.398 ± 17	339 ± 4	340 ± 12	351 ± 87
CS 52r-15	258	64	3672	0.0928 ± 30	0.0791 ± 14	0.0926 ± 14	1.009 ± 25	571 ± 8	709 ± 13	1174 ± 37
CS 52r-16	642	87	1887	0.0411 ± 31	0.0528 ± 14	0.0541 ± 7	0.394 ± 12	339 ± 4	337 ± 9	322 ± 58
CS 53r-1	458	81	18450	0.0556 ± 16	0.0533 ± 9	0.0543 ± 8	0.399 ± 9	341 ± 5	341 ± 7	341 ± 38
CS 53r-2	429	96	2474	0.0697 ± 33	0.0538 ± 15	0.0540 ± 8	0.400 ± 13	339 ± 5	342 ± 10	361 ± 63
CS 53r-3	632	33	6429	0.0166 ± 16	0.0540 ± 8	0.0537 ± 7	0.399 ± 9	337 ± 5	341 ± 7	370 ± 36
CS 53r-4	672	36	7851	0.0156 ± 16	0.0530 ± 8	0.0540 ± 8	0.394 ± 9	339 ± 5	337 ± 7	326 ± 36
CS 53r-5	590	14	7197	0.0094 ± 14	0.0533 ± 8	0.0541 ± 8	0.397 ± 9	339 ± 5	340 ± 7	342 ± 35
CS 53r-6	447	28	4148	0.0191 ± 20	0.0533 ± 10	0.0540 ± 8	0.397 ± 10	339 ± 5	339 ± 8	342 ± 45
CS 53r-7	569	44	5540	0.0242 ± 25	0.0538 ± 12	0.0558 ± 6	0.414 ± 11	350 ± 4	352 ± 8	362 ± 52
CS 53r-8-1	158	54	1478	0.1081 ± 70	0.0537 ± 31	0.0544 ± 6	0.403 ± 24	342 ± 4	344 ± 18	358 ± 126
CS 53r-8-2	2178	150	2758	0.0214 ± 12	0.0544 ± 6	0.0621 ± 8	0.465 ± 8	388 ± 5	388 ± 6	386 ± 24
CS 53l-9	262	136	886	0.1627 ± 71	0.0537 ± 30	0.0586 ± 7	0.434 ± 26	367 ± 4	366 ± 18	356 ± 125
CS 53r-10	290	85	1886	0.0906 ± 44	0.0528 ± 19	0.0542 ± 6	0.395 ± 16	340 ± 4	338 ± 12	321 ± 84
CS 53l-11	370	26	3325	0.0219 ± 24	0.0541 ± 12	0.0588 ± 7	0.439 ± 12	368 ± 4	369 ± 9	375 ± 53
CS 54r-1-1	797	44	6440	0.0174 ± 17	0.0539 ± 9	0.0540 ± 6	0.401 ± 8	339 ± 4	342 ± 6	366 ± 37
CS 54r-1-2	198	24	1360	0.0396 ± 101	0.0537 ± 43	0.0539 ± 7	0.399 ± 33	338 ± 5	341 ± 24	357 ± 175
CS 54r-2-1	396	35	2727	0.0297 ± 30	0.0537 ± 15	0.0539 ± 6	0.399 ± 12	338 ± 4	341 ± 9	358 ± 62
CS 54r-2-2	237	27	1435	0.0317 ± 55	0.0524 ± 23	0.0540 ± 7	0.391 ± 19	339 ± 5	335 ± 14	304 ± 102
CS 54r-3-1	275	29	2827	0.0312 ± 41	0.0529 ± 20	0.0537 ± 6	0.391 ± 16	337 ± 4	335 ± 12	325 ± 84
CS 54r-4-1	333	32	2825	0.0305 ± 45	0.0528 ± 21	0.0538 ± 6	0.392 ± 16	336 ± 4	338 ± 12	320 ± 89
CS 54r-4-2	750	52	3258	0.0206 ± 17	0.0532 ± 8	0.0539 ± 7	0.395 ± 8	338 ± 4	338 ± 6	337 ± 35
CS 54r-5-1	593	46	6905	0.0234 ± 23	0.0534 ± 11	0.0544 ± 6	0.401 ± 10	341 ± 4	342 ± 8	347 ± 49
CS 54r-5-2	465	32	3727	0.0226 ± 29	0.0531 ± 13	0.0545 ± 7	0.395 ± 11	339 ± 5	338 ± 9	331 ± 56
CS 54r-6-1	341	36	7573	0.0369 ± 33	0.0543 ± 16	0.0536 ± 6	0.401 ± 13	336 ± 4	342 ± 10	384 ± 66
CS 54r-6-2	123	21	1167	0.0554 ± 94	0.0531 ± 40	0.0542 ± 7	0.397 ± 31	340 ± 5	340 ± 23	335 ± 166
CS 54r-7	525	41	3123	0.0218 ± 27	0.0521 ± 13	0.0543 ± 6	0.390 ± 11	341 ± 4	334 ± 9	289 ± 58
CS 54r-8	709	39	3439	0.0183 ± 21	0.0533 ± 11	0.0461 ± 6	0.339 ± 8	290 ± 3	296 ± 6	343 ± 45
CS 54r-9	558	40	2139	0.0217 ± 29	0.0527 ± 14	0.0538 ± 6	0.391 ± 12	338 ± 4	335 ± 9	315 ± 60
CS 54r-10	342	31	5760	0.0260 ± 37	0.0520 ± 17	0.0546 ± 6	0.392 ± 14	343 ± 4	336 ± 11	287 ± 77
CS 54r-11	1138	60	4660	0.0167 ± 12	0.0534 ± 5	0.0541 ± 7	0.399 ± 7	340 ± 5	341 ± 6	347 ± 25
CS 54r-12	411	33	812	0.0248 ± 55	0.0531 ± 24	0.0542 ± 7	0.397 ± 19	340 ± 5	339 ± 14	333 ± 101
CS 54r-13	404	31	1081	0.0248 ± 55	0.0532 ± 24	0.0540 ± 7	0.396 ± 19	339 ± 14	339 ± 4	337 ± 100
CS 55r-1	118	56	2087	0.1494 ± 89	0.0530 ± 38	0.0536 ± 8	0.391 ± 29	337 ± 5	335 ± 22	327 ± 158

Table 1 (Contd.)

Sample no.[a]	U (ppm)	Th (ppm)	$^{206}Pb/^{204}Pb$	$^{208}Pb/^{206}Pb$	$^{207}Pb/^{206}Pb$	$^{206}Pb/^{238}U$	$^{207}Pb/^{235}U$	206/238 age ± 1σ	207/235 age ± 1σ	207/206 age ± 1σ
CS 55r-2	2249	187	24488	0.0245 ± 17	0.0533 ± 15	0.0540 ± 8	0.397 ± 13	339 ± 5	339 ± 10	342 ± 65
CS 55r-4	363	68	5979	0.0589 ± 21	0.0537 ± 10	0.0538 ± 7	0.399 ± 10	338 ± 5	341 ± 8	359 ± 44
CS 55r-5	115	33	2959	0.0909 ± 57	0.0534 ± 26	0.0536 ± 8	0.394 ± 20	336 ± 5	338 ± 15	346 ± 107
CS 55r-6	207	39	33327	0.0582 ± 13	0.0547 ± 9	0.0537 ± 7	0.398 ± 9	337 ± 5	340 ± 7	360 ± 38
CS 55r-7	179	35	3893	0.0594 ± 67	0.0530 ± 30	0.0538 ± 8	0.393 ± 23	338 ± 5	336 ± 17	327 ± 124
CS 55r-8	793	50	10560	0.0175 ± 24	0.0528 ± 11	0.0542 ± 8	0.394 ± 11	340 ± 5	338 ± 8	320 ± 49
CS 55r-10	1670	85	4200	0.0165 ± 13	0.0532 ± 6	0.0541 ± 7	0.397 ± 7	340 ± 5	340 ± 6	339 ± 26
CS 55r-11	165	31	470	0.0597 ± 118	0.0533 ± 50	0.0540 ± 8	0.397 ± 39	339 ± 5	340 ± 28	341 ± 203
CS 56r-1	131	23	4721	0.0591 ± 94	0.0541 ± 42	0.0540 ± 9	0.402 ± 31	339 ± 6	343 ± 24	375 ± 167
CS 56r-2	226	32	544662	0.0291 ± 5	0.1083 ± 7	0.2172 ± 36	3.243 ± 61	1267 ± 19	1467 ± 14	1771 ± 12
CS 56r-3	116	75	1389	0.1983 ± 111	0.0516 ± 47	0.0540 ± 9	0.384 ± 36	339 ± 6	330 ± 26	270 ± 197
CS 56r-4	164	46	3160	0.0916 ± 67	0.0547 ± 30	0.0547 ± 9	0.412 ± 24	343 ± 6	351 ± 18	398 ± 119
CS 56r-5	158	3	2749	0.0041 ± 65	0.0541 ± 30	0.0539 ± 9	0.402 ± 24	338 ± 6	343 ± 18	377 ± 123
CS 56r-6	169	94	1887	0.1729 ± 85	0.0510 ± 36	0.0548 ± 9	0.385 ± 28	344 ± 6	331 ± 21	240 ± 156
CS 56r-7	578	109	8441	0.0612 ± 15	0.0540 ± 8	0.0545 ± 9	0.406 ± 96	342 ± 6	346 ± 7	372 ± 34
CS 56r-8	133	23	2708	0.0540 ± 64	0.0539 ± 29	0.0754 ± 12	0.560 ± 33	469 ± 8	452 ± 22	366 ± 120
CS 56r-9	303	23	3411	0.0236 ± 39	0.0529 ± 18	0.0548 ± 9	0.400 ± 16	344 ± 6	342 ± 12	326 ± 79
CS 56r-10	964	63	4877	0.0179 ± 14	0.0553 ± 7	0.0755 ± 12	0.576 ± 12	469 ± 7	462 ± 8	432 ± 29
CS 56r-11	1222	37	8298	0.0098 ± 10	0.0536 ± 6	0.0546 ± 9	0.404 ± 8	343 ± 6	344 ± 6	355 ± 26
CS 56r-12	1712	167	35993	0.0325 ± 10	0.0546 ± 6	0.0542 ± 8	0.400 ± 8	340 ± 5	342 ± 6	353 ± 25
CS 57r-1	124	4	205381	0.0072 ± 7	0.0530 ± 10	0.0475 ± 7	0.347 ± 8	299 ± 4	303 ± 7	329 ± 44
CS 57r-2-1	233	9	11835	0.0122 ± 26	0.0534 ± 12	0.0543 ± 8	0.400 ± 11	341 ± 5	341 ± 9	344 ± 53
CS 57r-2-2	269	26	984	0.0324 ± 75	0.0537 ± 32	0.0542 ± 7	0.401 ± 25	340 ± 5	343 ± 19	360 ± 132
CS 57r-2-3	385	28	1048	0.0234 ± 61	0.0537 ± 26	0.0539 ± 7	0.400 ± 21	339 ± 5	341 ± 15	359 ± 109
CS 57r-3	167	5	9731	0.0084 ± 13	0.0528 ± 9	0.0538 ± 7	0.392 ± 9	338 ± 5	336 ± 7	322 ± 40
CS 57r-4	159	57	14229	0.1118 ± 20	0.0531 ± 9	0.0540 ± 8	0.395 ± 9	339 ± 5	338 ± 7	335 ± 41
CS 57r-5	89	5	9954	0.0143 ± 18	0.0525 ± 12	0.0536 ± 7	0.388 ± 11	337 ± 5	333 ± 8	308 ± 53
CS 57r-6	184	95	13488	0.1587 ± 24	0.0534 ± 9	0.0473 ± 7	0.348 ± 8	298 ± 4	303 ± 7	348 ± 41
CS 57r-7	129	7	13159	0.0195 ± 72	0.0544 ± 32	0.0540 ± 8	0.405 ± 25	339 ± 5	345 ± 18	387 ± 128
CS 57r-8	447	138	11707	0.0959 ± 38	0.0529 ± 17	0.0541 ± 7	0.395 ± 14	338 ± 10	339 ± 4	326 ± 71
CS 57r-9	349	16	20980	0.0160 ± 14	0.0541 ± 10	0.5405 ± 7	0.403 ± 9	344 ± 7	339 ± 4	374 ± 40
CS 57r-10	799	44	36329	0.0182 ± 7	0.0532 ± 6	0.0547 ± 7	0.401 ± 7	342 ± 5	343 ± 4	337 ± 24
CS 57r-11	1489	32	14235	0.0057 ± 13	0.0533 ± 7	0.0538 ± 6	0.396 ± 7	338 ± 5	338 ± 4	341 ± 30
CS 57r-12	380	16	983	0.0140 ± 50	0.0534 ± 22	0.0542 ± 7	0.398 ± 18	340 ± 5	341 ± 13	344 ± 92
CS 57r-13	808	41	2225	0.0144 ± 24	0.0531 ± 11	0.0538 ± 7	0.394 ± 10	338 ± 4	337 ± 7	331 ± 46
CS 57r-14	210	15	564	0.0233 ± 88	0.0530 ± 38	0.0541 ± 7	0.396 ± 30	340 ± 5	338 ± 21	328 ± 156

[a] r denotes round, multifaceted, metamorphic grain; l denotes long prismatic, magmatic grain; p denotes short prismatic, magmatic grain; 1-1 is spot 1 on grain 1, 1-2 is spot 2 on grain 1, etc

BSE images are very similar, except that dark areas in CL are bright in BSE, and vice versa. Some subtleness in zonation is often visible in one but not the other, and we found in our zircons from southern Bohemia that CL usually shows more detail than BSE. Both techniques are particularly useful in identifying different growth phases within zircons and to recognize inherited cores and overgrowth patterns (e.g. Vavra 1990; Hanchar and Miller 1993; Vavra et al. 1996).

Although the internal growth pattern in igneous zircons has been documented in numerous cases (e.g. Pidgeon 1992; Vavra 1994 for examples and literature), there are relatively few cases of well-described metamorphic zircons (e.g. Hoffmann and Long 1984; Vavra et al. 1996; Kröner and Willner 1998). Vavra et al. (1996) illustrate and describe the internal structure of near-spherical, multifaceted zircons from pelitic and psammitic metasediments of the Ivrea Zone, Italy, and our South Bohemian metamorphic zircons have much in common with these features. Typical is a well-developed sector zoning (Hoffman and Long 1984) as illustrated in Fig. 2. Growth sectors radiating outwards from the cores and with zigzag and "butterfly" shapes were also observed (Fig. 2, top). Vavra et al. (1996) relate such patterns to abrupt changes in the zircon growth rate, probably caused by small environmental changes such as temperature or variations in supersaturation of crystallizing particles. In most cases, the observed growth morphologies follow each other without any intermittent resorption event, similar to the Ivrea zircons as described by Vavra et al. (1996), but there are also rare examples where rounded surfaces cut the internal growth bands, suggesting that resorption has occurred (Fig. 2, top). Surprisingly, relatively few cases were observed where metamorphic zircons contained inherited cores.

Geochronology

We now present and discuss the individual results of the SHRIMP II spot analyses in combination with our

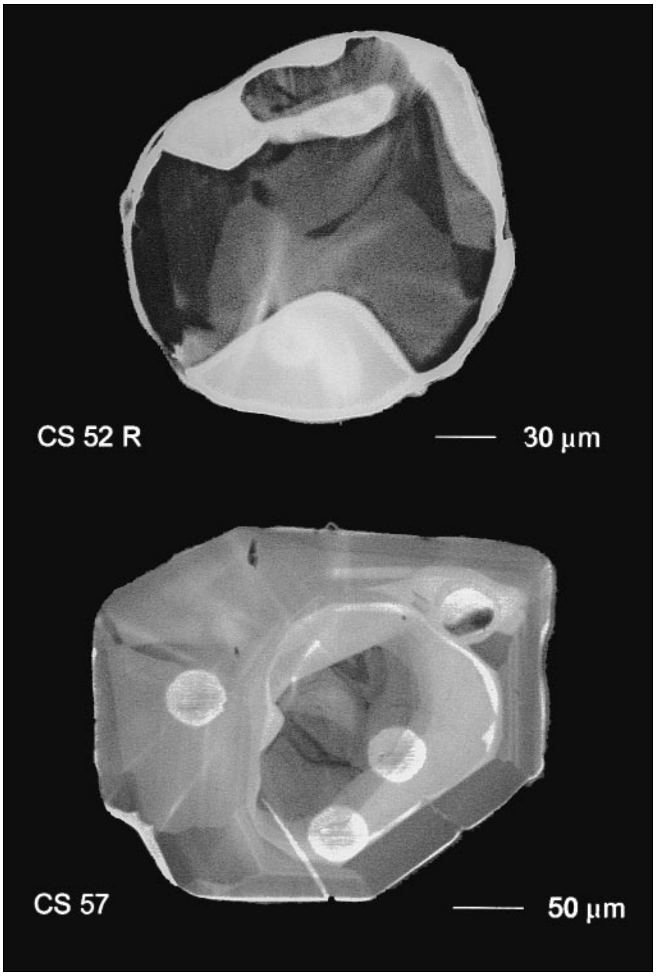

Fig. 2 Cathodoluminescence photograph showing internal structure of metamorphic zircons from granulite sample CS 52 (*top*) and CS 57 (*bottom*). Note "butterfly" pattern in top grain where the internal growth bands are cut by rounded surfaces, suggesting that resorption has occurred. *White spots* in bottom grain are burn marks of the ion microprobe

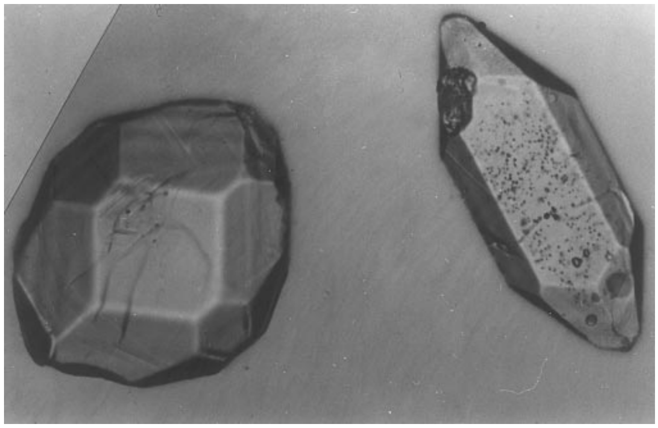

Fig. 3 Transmitted light photograph of multifaceted metamorphic zircon (*left*) and igneous zircon (*right*) from granodioritic gneiss sample CS 53, Kobylí hora quarry, Prachatice granulite massif, South Bohemia. Width of photograph is 300 μm

cathodoluminescence study. Sample CS 51 (felsic granulite, Kobylí hora, Fig. 1) contained abundant clear, spherical or near-spherical, metamorphic zircons (Fig. 3) ranging in diameter between about 30 and 120 μm as well as clear, long-prismatic, magmatic zircons with well-rounded terminations. CL and BSE imagery of the metamorphic zircons revealed a few cases of tiny (diameter less than 20 μm) cores surrounded by wide metamorphic overgrowth with sector zoning, but most grains are core-free and have two to three growth zones. Two grains were found where the innermost growth zones were cut by a wide outer zone of overgrowth, probably indicating significant resorption between the two phases.

Eight metamorphic grains were analysed (Table 1), all of them concordant and combining to a mean $^{206}Pb/^{238}U$ age of 341.0 ± 3.3 Ma (Fig. 4a), interpreted to reflect the time of metamorphic zircon growth during granulite-facies metamorphism. Four of these contained inherited cores that provided concordant $^{206}Pb/^{238}U$ ages of 360 ± 2 (mean of two grains), 399 ± 6 and 441 ± 6 Ma respectively (Table 1, Fig. 4a). This age spectrum of the inherited cores is also reflected in three analyses of the long prismatic grains (not shown in Fig. 4a) which provided concordant $^{206}Pb/^{238}U$ ages of 357 ± 2 (mean of two grains) and 408 ± 6 Ma respectively.

Sample CS 52, also from the Kobylí hora quarry, is from an in situ cordierite-bearing melt patch, cutting the earlier foliation, within a retrograded felsic granulite. This sample contains abundant clear, multifaceted grains with well-developed sector zoning as well as short prismatic, magmatic zircons and only rare cores. Twenty grain spots were analysed on SHRIMP II, and all analyses except one are concordant (Table 1, Fig. 4b). The 17 concordant metamorphic and short prismatic grains combine to a mean $^{206}Pb/^{238}U$ age of 340.4 ± 2.9 Ma, while the discordant grain (CS 52r-8, not plotted in Fig. 4b) probably lost Pb in recent times. One core analysis of a short-prismatic grain yielded an age of 421 ± 6 Ma (Fig. 4b). Two cores were much older, but the result is so discordant that the $^{207}Pb/^{206}Pb$ minimum ages of 879 ± 39 and 1174 ± 37 Ma (grains CS 52r-13 and 15, Table 1, not shown in Fig. 4b) are merely an indication of the Precambrian origin of this material. The short prismatic, magmatic grains from the cordierite-bearing melt pods are indistinguishable in age from the spherical grains. The metamorphic age is identical to that provided by zircons in sample CS 51, whereas the core age fits into the range of pre-metamorphic ages found in sample CS 51.

Sample CS 53, also from the Kobylí hora quarry, is from a granodioritic gneiss in direct contact with the granulites. This rock is strongly foliated at its margin but contains no melt patches. The rock contains both round, metamorphic grains (Fig. 3) with internal structures similar to those in samples CS 51 and 52, as well as long prismatic, magmatic grains (Fig. 3) with slightly to

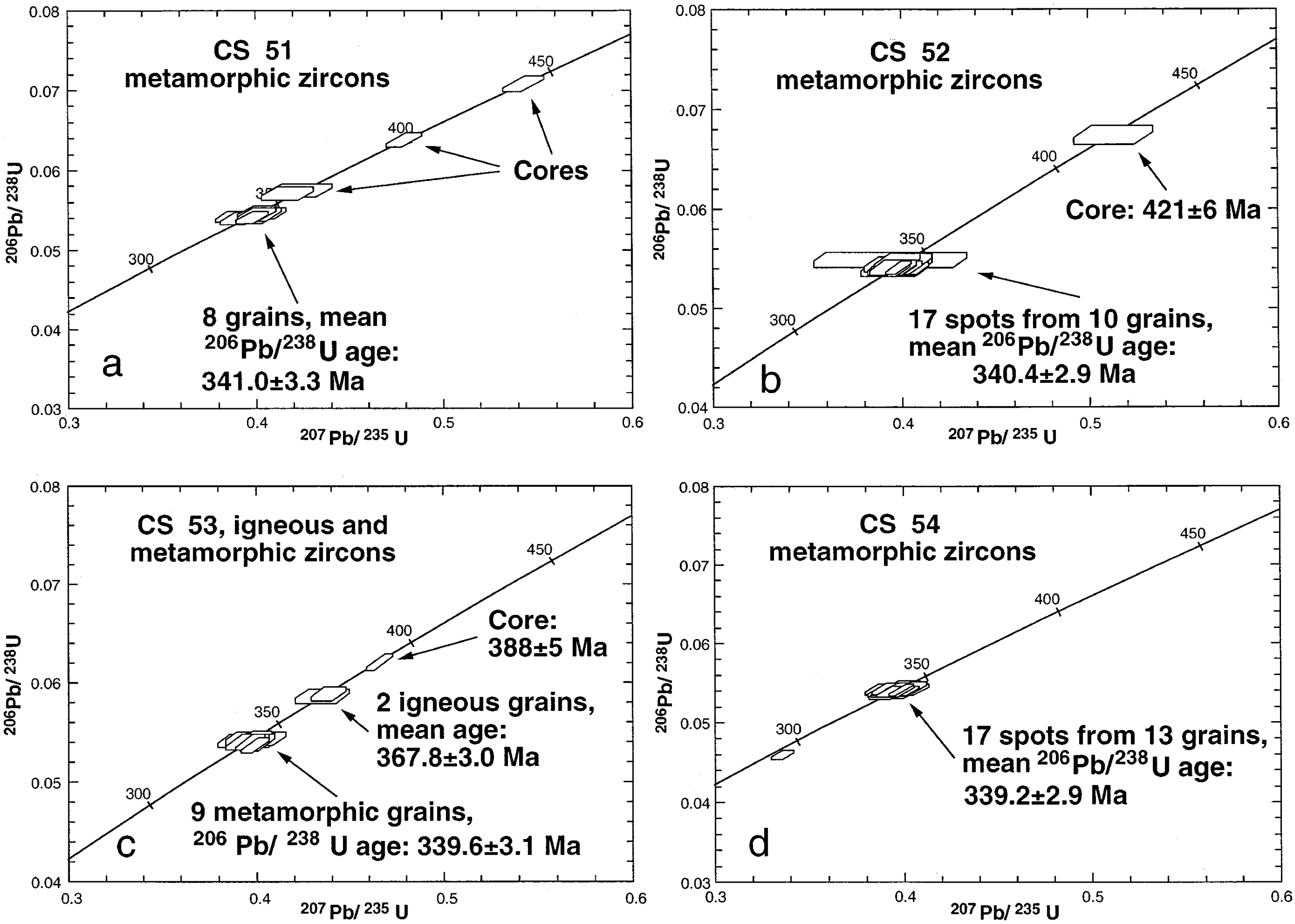

Fig. 4a–d Concordia diagrams showing SHRIMP II analyses of zircons from high-grade rocks of the Kobylí hora locality, Prachatice granulite massif, South Bohemia. Data boxes for each analysis are defined by standard errors in $^{207}Pb/^{235}U$, $^{206}Pb/^{238}U$ and $^{207}Pb/^{206}Pb$. **a** Metamorphic zircons from granulite sample CS 51. **b** Metamorphic zircons from granulite sample CS 52. **c** Igneous and metamorphic zircons from granodioritic gneiss sample CS 53. **d** Metamorphic zircon from granulite sample CS 54

well-rounded terminations and typical magmatic internal zonation such as described by Vavra (1994). All SHRIMP analyses are concordant (Table 1, Fig. 4c). Nine spots of the metamorphic grains combine to a mean $^{206}Pb/^{238}U$ age of 339.6 ± 3.1 Ma, while two igneous grains have a mean $^{206}Pb/^{238}U$ age of 367.8 ± 3.0 Ma (Fig. 4c). The core within one metamorphic grain has an age of 388 ± 5 Ma (Fig. 4c). The important implications arising from the results of this sample will be discussed below.

Sample CS 54, the last one from the Kobylí hora quarry, contains planar zones with sillimanite between less deformed domains in the rock. This rock contains almost exclusively clear, round, multifaceted zircons with well-developed sector zoning but no cores visible in CL or BSE. Up to four zones of zircon growth were observed in some grains (Fig. 3b). A total of 18 grain spots were analysed of which 17 were concordant, while one spot that was about 20% discordant (Table 1, Fig. 4d) we discard from further consideration. The mean $^{206}Pb/^{238}U$ age for 17 spot analyses from 13 grains is 339.2 ± 2.9 Ma, again identical to the ages of metamorphic zircons from the other samples of this quarry.

Sample CS 55 is a felsic granulite from the Lom pod Libínem quarry near Prachatice showing early stages of platy quartz development, kyanite grains rimmed by spinel, and cross-cutting patches of cordierite. The zircons are predominantly of the clear, near-spherical, multifaceted type with sector zoning, but there are also short prismatic morphologies with well-rounded terminations and significant structureless overgrowth as shown by CL and BSE imagery. Nine spots were analysed on the metamorphic grains and all yielded concordant results (Table 1) that combine to a mean $^{206}Pb/^{238}U$ age of 338.2 ± 3.2 Ma (Fig. 5a).

Sample CS 56 comes from the forest at Bulovy Hill in the Blanský les Massif (Fig. 1) where early structures are less overprinted by D_3-related refoliation and retrogression (Fiala 1992). The sample is from a thin lens (boudin) of felsic granulite within migmatite-like garnetiferous gneiss. The felsic granulite is considered to be anatectically derived from the surrounding migmatitic gneisses (cf. Vrána and Jakeš 1982; Vrána 1990; Fiala 1992). Only round, multifaceted, metamorphic zircons

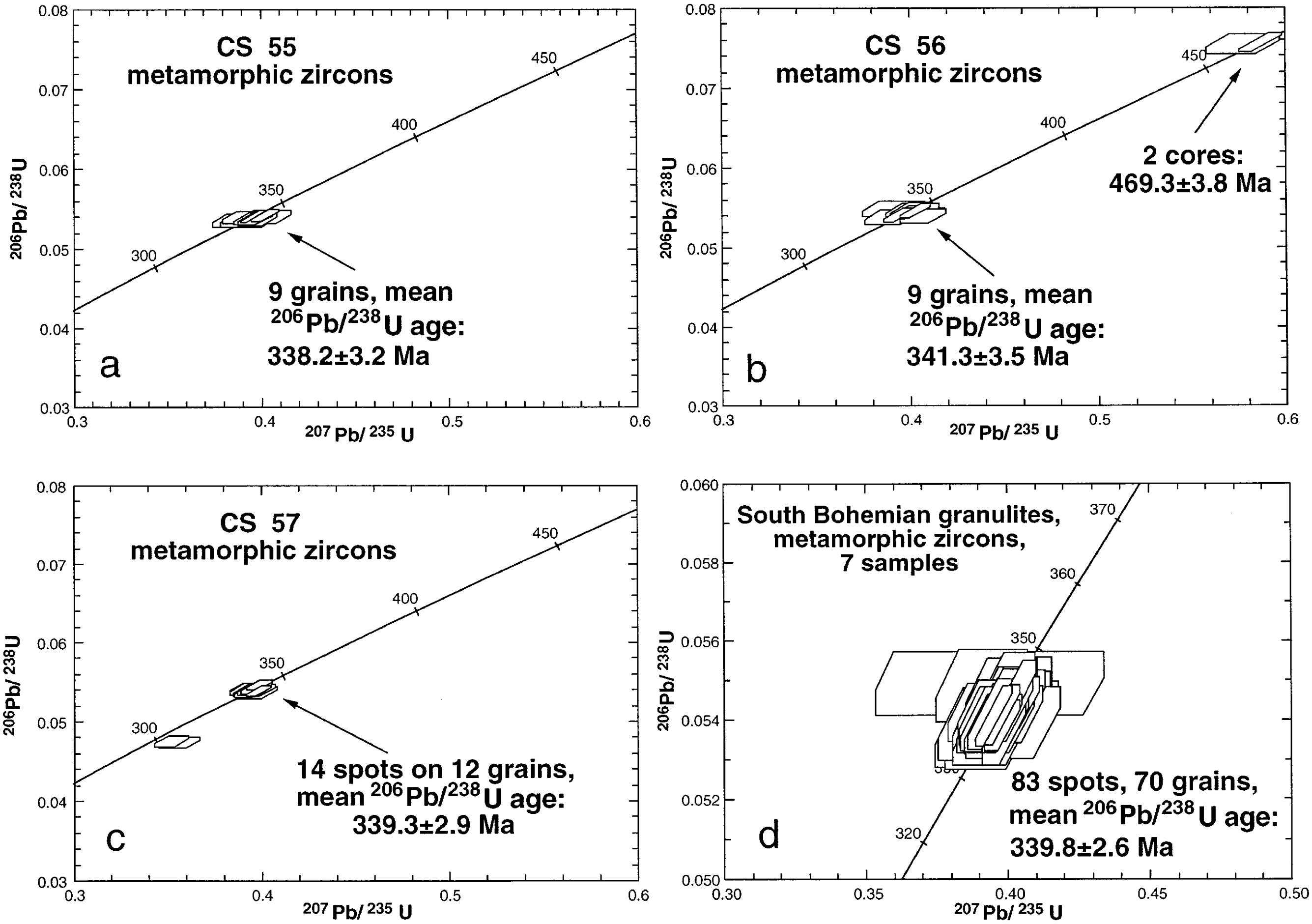

Fig. 5a–d Concordia diagrams showing SHRIMP II analyses of zircons from high-grade rocks of the Prachatice and Blanský les granulite massifs, South Bohemia. Data boxes as in Fig. 4. **a** Metamorphic zircons from granulite sample CS 55, Lom pod Libínem locality, Prachatice massif. **b** Metamorphic zircons from granulite sample CS 56, Bulovy Hill locality, Blanský les massif. **c** Metamorphic zircons from granulite sample CS 57, Bulovy Hill locality, Blanský les massif. **d** Summary diagram of 83 spot analyses from 70 metamorphic grains of samples CS 51–57

were analysed from this rock that show the same internal structures as zircons in the previous samples and reveal a few small cores under CL. All analyses except one are concordant (Table 1), and nine spots from the metamorphic grain domains combine to a mean $^{206}Pb/^{238}U$ age of 341.3 ± 3.5 Ma, while two cores have identical ages with a mean at 469.3 ± 3.8 Ma (Fig. 5b). One additional core (grain CS 56r-2) yielded a grossly discordant $^{207}Pb/^{206}Pb$ age of 1771 ± 13 Ma (Table 1, not shown in Fig. 5b) but, as in the case of sample CS 52, this is a minimum age and probably reflects the presence of some old pre-Variscan basement beneath the Blanský les Massif.

Lastly, sample CS 57, from the same outcrop as CS 56, represents the migmatitic, garnet- and (mostly secondary) biotite-rich gneiss (also kyanite and mesoperthite-bearing) from which the felsic granulite (sample CS 56) may be derived. It contains an abundance of clear, round, multifaceted zircons with no older cores but various layers of conformable growth. Sixteen grain spots were analysed of which two were about 15% discordant (Table 1) and were discarded. The remaining 14 analyses yield a mean $^{206}Pb/^{238}U$ age of 339.3 ± 2.9 Ma (Fig. 5c), again identical to the mean metamorphic ages calculated for all other samples.

If the analyses representative for metamorphic grain domains in all seven samples are considered together, this yields 83 spots derived from 70 grains, and the mean $^{206}Pb/^{238}U$ age is 339.8 ± 2.6 Ma (Fig. 5d).

Formation of metamorphic zircon at HT–HP and its significance as a chronometer

The closure temperature of zircon for the U–Pb system is probably well above 900 °C (e.g. Mezger and Krogstad 1997 and references therein) as documented by the survival of zircon xenocrysts in a variety of igneous rocks, notably basalt (Compston et al. 1986). Zircon can also survive regional metamorphism and partial melting (e.g. Gulson and Krogh 1973; Pankhurst and Pidgeon 1976; Harrison et al. 1987) . The experimental determination of diffusion parameters for U, Th, Pb and Hf in zircon (e.g. Cherniak et al. 1997; Lee et al. 1997) also support a very high closure temperature for the U–Pb system. This makes it almost certain that metamorphic zircon records the isotopic composition near or at its growth stage. Inclusion–host relationships, such as phengite in zircon (Kröner and Willner 1998) or isotopically almost undisturbed zircon in diamond from ultra-high pressure metamorphic rocks (Claoué-Long et al. 1991), can be used to constrain the age of zircon growth to parts of the metamorphic history. Ovoid to spherical, multifaceted zircons that grew during the pressure maximum are known from crustal ultra-high pressure rocks in the Kokchetav Massif, Kazakhstan (Claoué-Long et al. 1991; Sobolev et al. 1992) and in the Dora Maira Massif, Western Alps (Gebauer et al. 1993; Schertl and Schreyer 1995). In these rocks, phases that were stable near maximum pressure conditions, such as diamond, Si-rich phengite, jadeite-rich clinopyroxene, kyanite, pyrope, talc, coesite or rutile, were found enclosed within the zircons. Concordant U–Pb SHRIMP ages for such zircons were therefore interpreted as dating the peak of pressure, and the observed highly variable diffusive lead loss is probably due to the very short exposure of such rocks to extreme depths. Furthermore, closure of zircon to Pb diffusion in these rocks probably occurred at about the same time as closure of garnet and clinopyroxene to Nd diffusion (Mezger and Krogstad 1997). These two factors together, resistance to resetting and protection of inclusions, make metamorphic zircon probably the best currently available mineral to allow precise dating of regional high-grade metamorphism (Krogh 1993; Kröner and Jaeckel 1995; Mezger and Krogstad 1997).

Following zircon formation, the diffusive modification of zircon isotopic patterns under known crustal metamorphic conditions and time scales is unlikely (Cherniak et al. 1997; Lee et al. 1997), but the causes and timing of possible zircon dissolution, recrystallization or new growth must still be evaluated. Dissolution and growth of zircons under high-grade metamorphic conditions should be strongly influenced by the presence of alkali elements such as K and Na and by water- and pH-dependent cation solution reactions with the metamorphic fluid such as:

$$ZrSiO_4 + 4H^+ = Zr^{4+} + 2H_2O + SiO_2$$

Lowering the water activity or pH would enhance the solubility of zircon, but also rapid pressure–temperature changes may have a strong effect on the dissolution/precipitation behaviour. In general, all felsic metamorphic rocks that still preserve phases with compositions frozen at the PT-peak of HP–HT metamorphism in the southern Bohemian granulites document reduced water activities. Even when secondary biotite occurs, the fluid influx could only have been for a very restricted time period (O'Brien 1999), but it is noticeable in the geochemical study of Fiala et al. (1987) on the same granulites that secondary biotite presence can be directly correlated to whole-rock Zr, Th and U concentrations. This leads to the possibility that zircon growth is related to the influx of fluids that are required to produce biotite, i.e. at conditions far removed from the high pressure granulite stage. The analysed zircons that were drilled from thin sections, however, do not support a simple relationship between biotite growth and metamorphic zircon presence as the metamorphic type also occurs totally enclosed in large antiperthite grains. Likewise, the large idiomorphic zircons in the study of Aftalion et al. (1989) were sampled from inside garnet, a high-pressure phase.

The question of a possible relationship between melt presence and zircon growth in granulites was addressed by Roberts and Finger (1997). They proposed that, under the conditions of metamorphism deduced for felsic granulites of the Bohemian Massif (>900 °C, >15 kbar), there should have been melt present, and that the solubility of Zr in such a melt would be so high (based on the experimental data of Watson and Harrison 1983) that virtually all the zircons in the granulite protolith would have been dissolved in the melt. Zircon crystallization would then only take place as the rock evolution passed to conditions where lower water activity and Zr saturation in the melt occurred, i.e. at lower pressures. For this explanation to apply to the widespread ca. 340 Ma zircon age in the granulites (Table 2) we would need to identify textural sites of melt crystallization and be able to distinguish ages of these zircons from others (which would have to be the older, long prismatic or detrital types) in the rock. The evidence so far, however, is that the ca. 340 Ma spherical zircons can be found in the phases present at the high-pressure stage (garnet, ternary feldspar). Likewise, the zircons of the Zr-rich perpotassic granulite dated by Aftalion et al. (1989) were also found in the high-pressure phases. Taking, in addition, the evidence from the prismatic zircons in the cordierite-bearing melt spots measured in this study, it only strengthens the case for high, medium and low pressure granulite facies stages to have occurred within the time scale of the error of the SHRIMP analysis at around 340 Ma.

Conclusions

The results from zircon analysis for the South Bohemian granulites, including data from petrologically well-controlled grains drilled out of thin sections, are emphatic: the overwhelming majority of zircons are of metamorphic type, concordant at $\sim$340 Ma. The few cores identified in these zircons as well as long prismatic grains from the same rocks all yield older ages, with ca. 360 Ma being the youngest. These new results are in excellent agreement with those from previous granulite studies in the same area (van Breemen et al. 1982; Aftalion et al. 1989; Wendt et al. 1994; see Table 2) as well as elsewhere in the Bohemian Massif (Schenk and Todt 1983; von Quadt 1993; Friedl et al. 1994; Kotková et al. 1996; Becker 1997; Kröner and Willner 1998; Kröner et al. 1998; see Table 2). Most interesting are the results from the cordierite-bearing low-pressure melt pods cutting the

Table 2 Summary of known peak P-T ages for HP–HT rocks in the Bohemian Massif. Superscript numbers refer to references given in last column

Locality	U/Pb age of metamorphic zircons	Rock type	Sm/Nd whole-rock mineral isochron	Rock type	Reference
Granulite Massif (Saxony)	338 ± 4[1]	Garnet pyroxenite	380 ± 14[1]	Garnet pyroxenite	[1]von Quadt (1993) [2]Kröner et al. (1998)
	342 ± 4[1]	Felsic granulite	335 ± 4/346 ± 2[1]	Felsic granulite	
	352 ± 2[1]	Mafic granulite	308 ± 9[1]	Mafic granulite	
	340 ± 4[2]	Felsic granulites			
Erzgebirge (Saxony/Czech Republic)	341 ± 1[1]	Felsic granulite	333 ± 7[4]	Eclogite	[1]Kröner and Willner (1998) [2]Kotková et al. (1996) [3]Gebauer (1991) [4]Schmädicke et al. (1995)
	342 ± 1[1]		366 ± 4[4]		
	340 ± 1[1]		337 ± 5[4]		
	339 ± 1[2]				
	348 ± 10[2]				
	342 ± 5[3]	Garnet peridotite	353 ± 7[4]	Garnet pyroxenite	
Münchberg Gneiss Massif (Bavaria)	380 +14/−22[1]	Eclogite	395 ± 4[2]	Eclogite	[1]Gebauer and Grünfelder (1979) [2]Stosch and Lugmair (1990)
Oberpfalz (Bavaria)			424 ± 10	Eclogite	von Quadt and Gebauer (1993)
			424 ± 13	Granulite	
Dunkelsteiner Wald (Austria)	339.8 ± 1.1[1]	Charnockite	344 ± 10[2]	Garnet pyroxenite	[1]O'Brien and Kröner (unpublished) [2]Carswell and Jamtveit (1990)
			370 ± 15[2]		
Gföhl Nappe Blansky les Massiv, (S Bohemia)	338 ± 1	Perpotassic granulite			Aftalion et al. (1989)
	346 ± 12	Mafic granulite	343 ± 21	Mafic granulite	Wendt et al. (1994)
	341.1 ± 2.4	Felsic granulites			Kröner et al. (1996)
			327 ± 19	Garnet cpxenite	Medaris et al. (1995)
Lisov Massif (S Bohemia)	347, 357	Granulite			Van Breemen et al. (1982)
Gföhl Nappe (W Moravia)	347 ± 9[3]	Felsic granulite	341 ± 7[1]	Eclogite	[1]Brueckner et al. (1991) [2]Beard et al. (1992) [3]Kröner et al. (1988)
			373 ± 7[1]		
			324 ± 5[1]		
			323 ± 7[2]	Eclogite	
			336 ± 16[2]		
			342 ± 9[2]		
Kutná Hora-Svratka (Central Bohemia)			338 ± 6[1]	Eclogite	[1]Brueckner et al. (1991) [2]Beard et al. (1992) [3]Medaris et al. (1995)
			377 ± 20[2]		
			338 ± 8[3]	ky-eclogite	
			337 ± 6[3]	Eclogite	
Mariánské Lázne Complex (NW Bohemia)			377 ± 7	Eclogite	Beard et al. (1995)
			367 ± 4	Eclogite	Beard et al. (1995)
Góry Sowie (Polish Sudetes)	402 ± 1[1]	Mafic granulite	402 ± 3[2]	Garnet peridotite	[1]O'Brien et al. (1997a) [2]Brueckner et al. (1996)
Snieznik Mts (Polish Sudetes)			352 ± 4	Mafic granulite	Brueckner et al. (1991)
			341 ± 7	Eclogite	
			329 ± 6		
			352 ± 4		

main fabric where the age of the magmatic zircon cannot be distinguished from the metamorphic type in the same sample. This can be directly compared to the 338 + 1/−2 age of a large magmatic zircon included in high-pressure garnet from a perpotassic granulite of the Blanský les complex (Aftalion et al. 1989). All results point to the same age for zircon of metamorphic and magmatic origin regardless of whether melting was related to the initial high pressure stage or whether it was part of the late low pressure evolution.

The multifaceted zircons found in the meta-granodiorite, a rock whose emplacement must post-date the high-pressure metamorphism and most of the strong mylonitization on petrographic grounds, are identical to those in the granulites. This must mean that the granodiorite was produced by melting of granulite, or of a rock with the same zircon type and age distribution, and has incorporated the zircons without morphological and isotopic modification. It would mean, however, that in this sample we failed to identify magmatic zircons formed at 340 Ma during the melting event (as in the cordierite-bearing rock) or later. The alternative is that the prismatic grains in the meta-granodiorite (368 Ma) record the magmatic stage in the rock, and the abundant metamorphic grains formed during the granulite facies metamorphism as in the surrounding rocks but without textural or mineralogical alteration (biotite would have to remain unaffected by 1000 °C temperatures!). This seems highly unlikely.

The petrological study of the granulites revealed a metamorphic history with at least three high-temperature stages that occurred at significantly different temperatures. High-pressure conditions, above those expected in the normal continental crust, are confirmed by the initial garnet–clinopyroxene–plagioclase–quartz and garnet–ternary feldspar–kyanite–quartz assemblages of the mafic and felsic granulites respectively and correspond directly to results from other Bohemian Massif granulites (Carswell and O'Brien 1993; Kotková et al. 1996; O'Brien et al. 1997a; Willner et al. 1997; see Table 2). Orthopyroxene growth in the mafic granulite took place under medium pressure granulite facies conditions, and lower pressure conditions for overprints in the felsic granulites are suggested by garnet zonation to lower rim Ca, spinel after aluminosilicate and later cordierite growth. All petrological evidence indicates that the high, medium and low pressure stages occurred at high temperatures. The two distinct garnet domains or growth stages have also been noted in granulites from elsewhere in the Bohemian Massif (Owen and Dostal 1996; Willner et al. 1997), and the presence of corundum and/or spinel (and/or sapphirine) in Ca-rich domains surrounded by corona garnet (and the subsequent breakdown of the phases in these domains) have also been the subject of discussion (Carswell et al. 1989; Becker and Altherr 1991; Carswell and O'Brien 1993; Petrakakis and Jawecki 1995). There is no reason to believe, on petrological or geochronological grounds, that there is any difference in geologic evolution between the felsic granulites from Bohemia, Lower Austria, Saxony, or the Sudetes in the Bohemian Massif, or even from the Variscan basement of the Vosges farther west (van Breemen et al. 1982; Aftalion et al. 1989; Brueckner et al. 1991; von Quadt 1993; Wendt et al. 1994; Medaris et al. 1995; Kotková et al. 1996; Kröner and Willner 1998; Kröner et al. 1998). The only investigated high pressure granulites without a recognizable 340 Ma zircon component are those from the Sowie Góry (Owl Mountains) in the Polish Sudetes (O'Brien et al. 1997a; see Table 2), but even the metamorphic age of 400 Ma for these granulites is reflected in ages of zircon cores in the South Bohemian rocks (this study).

The granitic to granodioritic composition of the granulites (Fiala et al. 1987; Vellmer 1992) has a special significance. The rocks most likely represent the melt products of continental crust at mantle pressures (Vrána and Jakeš, 1982; Vrána 1989). Important to recognize in this respect is the poikiloblastic form of garnet (or clinopyroxene in more intermediate bulk compositions), with many of the inclusions being large mesoperthite grains. Also, it is not unusual to see corona growth of garnet around idiomorphic feldspar grains in these rocks – clearly a magmatic rather than a metamorphic (solid-state) feature. The poikiloblastic texture is characteristic for garnets grown during incongruent melting reactions such as biotite + plagioclase + aluminosilicate + quartz = garnet + K-feldspar + melt (biotite dehydration melting) in metapelites and has been documented from migmatite belts worldwide (e.g. Waters and Whales 1984; Le Breton and Thompson 1988). If the granulites were derived by melting of pelites, a considerable volume of restitic material (garnet + kyanite-rich) would also be expected. An alternative would be melting of an existing granite or granitic gneiss.

Acknowledgements We thank Hubert Schulze (Bayerisches Geoinstitut) for his careful extraction and preparation of the zircons from thin sections. Financial support (for A.K. and P.J.O.) by the Deutsche Forschungsgemeinschaft (DFG) within the priority programme "Orogenic Processes" is gratefully acknowledged. The zircon analyses were carried out on the Sensitive High Resolution Ion Microprobe mass spectrometer (SHRIMP II) operated by a consortium consisting of Curtin University of Technology, the Geological Survey of Western Australia and the University of Western Australia with the support of the Australian Research Council. We appreciate the advice of A. Kennedy and D. Nelson during SHRIMP analysis and data reduction. The comments of B. Beard and an anonymous reviewer led to considerable improvement of the original manuscript.

References

Aftalion M, Bowes DR, Vrana S (1989) Early Carboniferous U–Pb zircon age for garnetiferous perpotassic granulites, Blansky les massif, Czechoslovakia. Neues Jahrb Mineral Monatsh 4: 145–152

Arnold A, Scharbert HG (1973) Rb–Sr-Altersbestimmungen an Granuliten der südlichen Böhmischen Masse in Österreich. Schweiz Miner Petrol Mitt 53: 61–78

Beard BL, Medaris LG Jr, Johnson CM, Brueckner HK, Mísaø, Z (1992) Petrogenesis of Variscan high temperature Group A eclogites from the Moldanubian Zone of the Bohemian Massif, Czechoslovakia. Contrib Mineral Petrol 111: 468–483

Beard BL, Medaris LG Jr, Jelinek E, Tonika J, Riciputi LR (1995) Geochronology and geochemistry of eclogites from the Marianske Lazne Complex, Czech Republic: implications for Variscan orogenesis. Geol Rundschau 84: 552–567

Becker H (1997) Sm–Nd garnet ages and cooling history of high-temperature garnet peridotite massifs and high-pressure granulites from lower Austria. Contrib Mineral Petrol 127: 224–236

Becker H, Altherr R (1991) Al-rich sapphirine in a high-P charnockite: reaction textures and P–T-evolution. Terra Abstr 3: 437

Berman RG (1990) Mixing properties of Ca–Mg–Fe–Mn garnets. Am Mineral 75: 328–344
Berman RG (1991) Thermobarometry using multi-equilibrium calculations: a new technique with petrological applications. Can Mineral 29: 833–855
Brueckner HK, Medaris LG Jr, Bakun-Czubarow N (1991) Nd and Sr age and isotope patterns from Variscan eclogites of the eastern Bohemian Massif. N Jahrb Mineral Abh 163: 169–196
Brueckner HK, Blusztajn J, Bakun-Czubanov N (1996) Trace element and Sm–Nd age zoning in garnets from peridotites of the Caledonian and Variscan mountains and tectonic implications. J Metamorph Geol 14: 61–73
Brey GP, Köhler T (1990) Geothermobarometry in four-phase lherzolites II. New thermobarometers and practical assessment of existing thermobarometers. J Petrol 31: 1353–1378
Carswell DA, Jamtveit B (1990) Variscan Sm–Nd ages for the high-pressure metamorphism in the Moldanubian Zone of the Bohemian Massif, Lower Austria. N Jahrb Mineral Abh 162: 69–78
Carswell DA, O'Brien PJ (1993) Thermobarometry and geotectonic significance of high pressure granulites: examples from the Moldanubian Zone of the Bohemian Massif in Lower Austria. J Petrol 34: 427–459
Carswell DA, Miller C, O'Brien PJ (1989) Origin of sapphirine symplectites in metabasites from Mitterbachgraben, Dunkelsteinerwald granulite complex, Lower Austria. Eur J Mineral 1: 455–466
Cherniak DJ, Hanchar JM, Watson EB (1997) Diffusion of tetravalent cations in zircon. Contrib Mineral Petrol 127: 383–390
Claoué-Long JC, Sobolev NV, Shatsky VS, Sobolev AV (1991) Zircon response to diamond-pressure metamorphism in the Kokchetav massif, USSR. Geology 19: 710–713
Claoué-Long JC, Compston W, Roberts J, Fanning CM (1995) Two Carboniferous ages: a comparison of SHRIMP zircon dating with conventional zircon ages and $^{40}Ar/^{39}Ar$ analyses. Soc Sediment Geol, Spec Publ 54: 3–21
Compston W, Williams IS, Myer C (1984) U–Pb geochronology of zircons from Lunar Breccia 73217 using a sensitive high mass-resolution ion-microprobe. J Geophys Res 89 (Suppl) B525–B534
Compston W, Williams IS, Campbell IH, Gresham JJ (1986) Zircon xenocrysts from the Kambalda volcanics: age constraints and direct evidence for older continental crust below the Kambalda–Norseman greenstones. Earth Planet Sci Lett 76: 299–311
Compston W, Williams IS, Kirschvink JL, Zhang Z, Ma G (1992) Zircon U–Pb ages for the Early Cambrian time scale. J Geol Soc Lond 149: 171–184
Dallmeyer RD, Neubauer F, Höck V (1992) Chronology of late Paleozoic tectonothermal activity in the southeastern Bohemian Massif, Austria (Moldanubian and Moravo–Silesian zones): $^{40}Ar/^{39}Ar$ mineral age controls. Tectonophysics 210: 135–153
Ferry JM, Spear FS (1978) Experimental calibration of the partitioning of Fe and Mg between biotite and garnet. Contrib Mineral Petrol 66: 113–117
Fiala J (1992) Stop 5: Bulovy – evolution of granulites of the Blansky les massif. Excursion guide, International Workshop 'High Pressure Granulites – Lower Crustal Metamorphism', Rohanov, 27 June–5 July 1992, Czech Geological Survey, pp 16–17
Fiala J (1995) General characteristics of the Moldanubian Zone. In: Dallmeyer RD, Franke W, Weber K (eds) Pre-Permian geology of Central and Eastern Europe. Springer, Berlin Heidelberg New York, pp 417–418
Fiala J, Matejovska O, Vankova VB (1987) Moldanubian granulites: source material and petrogenetic considerations. Neues Jahrb Mineral Abh 157: 133–165
Frank W, Hammer S, Popp F, Scharbert S, Thöni M (1990) Isotopengeologische Neuergebnisse zur Entwicklungsgeschichte der Böhmischen Masse proterozoische Gesteinsserien und variszische Hauptorogenese. Österr Beitr Meteor Geophys 3: 185–228
Friedl G, von Quadt A, Ochsner A, Finger F (1993) Timing of the Variscan orogeny in the Southern Bohemian Massif (NE Austria) deduced from new U–Pb zircon and monazite dating. Terra Nova 5: 235–236
Friedl G, von Quadt A, Finger F (1994) 340 Ma U/Pb-Monazitalter aus dem niederösterreichischen Moldanubikum und ihre geologische Bedeutung. Terra Nostra 3/94: 43–46
Fuchs G (1971) Zur Tektonik des östlichen Waldviertels (Niederöserreich). Verh Geol Bundesanstalt Wien 3: 424–440
Fuchs G (1991) Das Bild der Böhmischen Masse im Umbruch. Jahrb Geol Bundesanstalt Wien 134: 701–710
Fuchs G (1995) The Austrian part of the Moldanubicum. In: Dallmeyer RD, Franke W, Weber K (eds) Pre-Permian geology of Central and Eastern Europe. Springer, Berlin Heidelberg New York, pp 422–426
Fuhrman ML, Lindsley DH (1988) Ternary-feldspar modelling and thermometry. Am Mineral 73: 201–215
Gebauer D (1991) Two Paleozoic high-pressure events in a garnet–peridotite of northern Bohemia, Czechoslovakia. Abstracts, 2nd Eclogite Field Symp, Granada, Terra Abstracts (Suppl 6 to Terra Nova) 3: 5
Gebauer D, Friedl G (1994) A 1.38 Ga protolith age for the Dobra Orthogneiss (Moldanubian Zone of the southern Bohemian Massif, NE-Austria): evidence from ion-microprobe (SHRIMP) dating of zircon. J Czech Geol Soc 39: 34–35
Gebauer D, Grünenfelder M (1979) U–Pb zircon and Rb–Sr mineral dating of eclogites and their country rocks. Example: Münchberg Gneiss Massif, northeast Bavaria. Earth Planet Sci Lett 42: 35–44
Gebauer D, Tilton GR, Schertl HP, Schreyer W (1993) Eocene/Oligocene ultrahigh-pressure (UHP)-metamorphism in the Dora Maira Massif (Western Alps) and its geodynamic implications. Terra Abstr (Suppl to Terra Nova) 5: 10–11
Gulson BL, Krogh TT (1973) Old lead components in the young Bergell Massif, south-east Swiss Alps. Contrib Mineral Petrol 40: 239–252
Hanchar JM, Miller CF (1993) Zircon zonation patterns as revealed by cathodoluminescence and backscattered electron images: implications for interpretation of complex crustal histories. Chem Geol 110: 1–13
Harrison TM, Aleinikoff JN, Compston W (1987) Observations and controls on the occurrence of inherited zircon in Concord-type granitoids, New Hampshire. Geochim Cosmochim Acta 52: 2549–2558
Hoffmann JF, Long JVP (1984) Unusual sector zoning in Lewisian zircons. Mineral Mag 48: 513–517
Hoppe G (1962) Petrogenetisch auswertbare morphologische Erscheinungen an akzessorischen Zirkonen. N Jahrb Mineral Abh 98: 35–50
Jaeckel P, Kröner A, Kamo SL, Brandl G, Wendt JI (1997) Late Archaean to early Proterozoic granitoid magmatism and high-grade metamorphism in the central Limpopo belt, South Africa. J Geol Soc Lond 154: 25–44
Kennedy AK, De Laeter JR (1994) The performance characteristics of the WA SHRIMP II ion microprobe. US Geol Surv Circ 1107: 166
Kinny PD (1986) 3820 Ma zircons from a tonalitic Amitsoq gneiss in the Godthab district of southern West Greenland. Earth Planet Sci Lett 79: 337–347
Konzalov M (1980) Zu der mikropaläontologischen Erforschung graphitischer Gesteine im Südteil der Böhmischen Masse. Vûst Úst Úst Geol 51: 233–236
Kotková J, Harley SL (1997) Mineral controls on the trace element and REE geochemistry of high-pressure leucogranulites from the Bohemian Massif. J Czech Geol Soc 42: 40
Kotková J, Kröner A, Todt W, Fiala J (1996) Zircon dating of North Bohemian granulites, Czech Republic: further evidence for the Lower Carboniferous high-pressure event in the Bohemian Massif. Geol Rundsch 85: 154–161
Koziol AM, Newton RC (1989) Grossular activity–composition relationships in ternary garnets determined by reversed displaced-equilibrium experiments. Contrib Mineral Petrol 103: 423–433

Krogh TE (1993) High precision U–Pb ages for granulite metamorphism and deformation in the Archean Kapuskasingm structural zone, Ontario: implications for structure and development of the lower crust. Earth Planet Sci Lett 119: 1–18

Kröner A, Jaeckel P (1995) Dating the peak of high-temperature regional metamorphism by using metamorphic zircons. EOS 76 (Suppl F703–704)

Kröner A, Willner AP (1998) Time of formation and peak of Variscan HP–HT metamorphism of quartz–feldspar rocks in the central Erzgebirge, Saxony, Germany. Contrib Mineral Petrol 132: 1–20

Kröner A, Wendt I, Liew TC, Compston W, Todt W, Fiala J, Vankova V, Vanek J (1988) U–Pb zircon and Sm–Nd model ages of high-grade Moldanubian metasediments, Bohemian Massif, Czechoslovakia. Contrib Mineral Petrol 99: 257–266

Kröner A, Jaeckel P, Williams IS (1994) Pb-loss patterns in zircons from a high-grade metamorphic terrain as revealed by different dating methods: U–Pb and Pb–Pb ages for igneous and metamorphic zircons from northern Sri Lanka. Precambrian Res 66: 151–181

Kröner A, Willner AP, Hegner E, Frischbutter A, Hofmann J, Bergner R (1995) Latest Precambrian (Cadomian) zircon ages, Nd isotopic systematics and P–T evolution of granitoid orthogneisses of the Erzgebirge, Saxony and Czech Republic. Geol Rundsch 84: 437–456

Kröner A, O'Brien PJ, Pidgeon RT (1996) SHRIMP zircon ages for HP–HT granulites from the Moldovian zone of southern Bohemia. EOS 77 (Suppl F820)

Kröner A, Jaeckel P, Reischmann T, Kroner U (1998) Further evidence for an early Carboniferous (~340 Ma) age of high-grade metamorphism in the Saxonian Granulite Complex. Geol Rundsch 86: 751–766

Le Breton N, Thompson AB (1988) Fluid-absent (dehydration) melting of biotite in metapelites in the early stages of crustal anatexis. Contrib Mineral Petrol 99: 226–237

Lee JKW, Williams IS, Ellis DJ (1997) Pb, U and Th diffusion in natural zircon. Nature 390: 159–161

Linner M (1996) Metamorphism and partial melting of the Monotonous Group, SE Moldanubicum (Austria). Mineral Petrol 58: 215–234

Medaris LG Jr, Beard BL, Johnson CM, Valley JW, Spicuzza MJ, Jelinek E, Mísar Z (1995) Garnet pyroxenite and eclogite in the Bohemian Massif: geochemical evidence for Variscan recycling of subducted lithosphere. Geol Rundsch 84: 489–505

Mezger K, Krogstad EJ (1997) Interpretation of discordant U–Pb zircon ages: an evaluation. J Metamorph Geol 15: 127–140

Nelson DR (1997) Compilation of SHRIMP U–Pb zircon geochronology data, 1996. Geol Surv Western Australia, Record 1997/2, 189 pp

Neumann W (1984) Zur erdgeschichtlichen Entwicklung des sächsischen Granulitmassivs. Z Angew Geol 30: 183–190

O'Brien PJ (1999) Asymmetric zoning profiles in garnet from HP–HT granulite and implications for volume and grain boundary diffusion. Mineral Mag 63: 227–238

O'Brien PJ, Vrána S (1995) Eclogites with a short-lived granulite facies overprint in the Moldanubian Zone, Czech Republic: petrology, geochemistry and diffusion modelling of garnet zoning. Geol Rundsch 84: 473–488

O'Brien PJ, Kröner A, Jaeckel P, Hegner E, Żelaźniewicz A, Kryza R (1997a) Petrological and isotopic studies on Palaeozoic high pressure granulites with a medium pressure overprint, Góry Sowie (Owl) Mts, Polish Sudetes. J Petrol 38: 433–456

O'Brien PJ, Duyster J, Grauert B, Schreyer W, Stöckhert B, Weber K (1997b) Crustal evolution of the KTB drill site: from oldest relics to the late Hercynian granites. J Geophys Res 102: 18203–18220

Owen JV, Dostal J (1996) Contrasting corona structures in mafic granulite from the Blansky les complex, Bohemian Massif, Czech Republic. Can Mineral 34: 959–966

Pacltov B (1994) Silurian (Wenlockian) sporomorph in South Bohemian Moldanubicum. J Czech Geol Soc 39: 81–82

Pankhurst RJ, Pidgeon RT (1976) Inherited isotope systems and the source region pre-history of early Caledonian granites in the Dalradian Series of Scotland. Earth Planet Sci Lett 31: 55–68

Paterson BE, Stephens WE, Herd DA (1989) Zoning in granitoid accessory minerals as revealed by backscattered electron imagery. Mineral Mag 53: 55–62

Petrakakis K, Jawecki C (1995) High-grade metamorphism and retrogression of Moldanubian granulites. Austria Eur J Mineral 7: 1183–1203

Pidgeon RT (1992) Recrystallisation of oscillatory zoned zircon – some geochronological and petrological implications. Contrib Mineral Petrol 110: 463–472

Pidgeon RT, Bowes DR (1972) U–Pb ages of granulites from the central region of the Lewisian, northwest Scotland. Geol Mag 109: 247–258

Pin C, Vielzeuf D (1983) Granulites and related rocks in Variscan median Europe: a dualistic interpretation. Tectonophysics 93: 47–74

Roberts MP, Finger F (1997) Do U–Pb ages from granulites reflect peak metamorphic conditions? Geology 25: 319–322

Rötzler J (1992) Zur Petrogenese im sächsischen Granulitgebirge. Die pyroxenfreien Granulite und die Metapelite. Geotekton Forsch 77: 1–100

Schenk V, Todt W (1983) U–Pb Datierungen an Zirkon und Monazit der Granulite im Moldanubikum Niederosterreichs (Waldviertel). Fortschr Miner 61: 190–191

Schertl HP, Schreyer W (1995) Mineral inclusions in heavy minerals of the ultrahigh-pressure metamorphic rocks of the Dora-Maira massif and their bearing on the relative timing of the petrological events. In: Basu A, Hart SR (eds) Earth processes: reading the isotopic code. AGU Monogr Ser 95: 331–342

Sobolev NV, Shatsky VS, Vavilov MA, Goryaynov SV (1992) A coesite inclusion in zircon from diamond-containing gneiss of the Kokchetav massif: the first find of coesite in metamorphic rocks of the USSR. Trans Russian Acad Sci (Earth Sci Sect) 322: 123–127

Stosch HG, Lugmair GW (1990) Geochemistry and evolution of MORB-type eclogites from the Münchberg Massif, southern Germany. Earth Planet Sci Lett 99: 230–249

van Breemen O, Aftalion M, Bowes DR, Dudek A, Mísar Z, Povondra P, Vrána S (1982) Geochronological studies of the Bohemian Massif, Czechoslovakia, and their significance in the evolution of Central Europe. Trans R Soc Edinburgh, Earth Sci 73: 89–108

Vavra G (1990) On the kinematics of zircon growth and its petrogenetic significance: a cathodoluminescence study. Contrib Mineral Petrol 106: 90–99

Vavra G (1994) Systematics of internal zircon morphology in major Variscan granitoid types. Contrib Mineral Petrol 117: 331–344

Vavra G, Gebauer D, Schmidt R, Compston W (1996) Multiple zircon growth and recrystallization during polyphase late Carboniferous to Triassic metamorphism in granulites of the Ivrea Zone (southern Alps): an ion microprobe (SHRIMP) study. Contrib Mineral Petrol 122: 337–358

Vellmer C (1992) Stoffbestand und Petrogenese von Granuliten und granitischen Gesteinen der südlichen Böhmischen Masse in Niederösterreich. Doctoral Thesis, University of Göttingen

von Quadt A (1993) The Saxonian Granulite Massif: new aspects from geochronological studies. Geol Rundsch 82: 516–530

von Quadt A, Gebauer D (1993) Sm–Nd and U–Pb dating of eclogites and granulites from the Oberpfalz, NE Bavaria, Germany. Chem Geol 109: 317–339

Vrána S (1979) Polyphae shear folding and thrusting in the Moldanubicum of southern Bohemia. Vest Ustr Ust Geol 54: 75–86

Vrána S (1990) Perpotassic granulites from southern Bohemia. A new rock-type derived from partial melting of crustal rocks under upper mantle conditions. Contrib Mineral Petrol 103: 510–522

Vrána S, Jakeš P (1982) Orthopyroxene and two-pyroxene granulites from a segment of charnockitic crust in southern Bohemia. Bull Geol Surv Prague 57: 129–143

Waters DJ, Whales CJ (1984) Dehydration melting and the granulite transition in metapelites from southern Namaqualand, S. Africa. Contrib Mineral Petrol 88: 269–275

Watson EB, Harrison TM (1983) Zircon saturation revisited: temperature and composition effects in a variety of crustal magma types. Earth Planet Sci Lett 64: 295–304

Wendt JI, Kröner A, Fiala J, Todt W (1993) Evidence from zircon dating for existence of approximately 2.1 Ga old crystalline basement in southern Bohemia, Czech Republic. Geol Rundsch 82: 42–50

Wendt JI, Kröner A, Fiala J, Todt W (1994) U–Pb zircon and Sm–Nd dating of Moldanubian HP/HT granulites from South Bohemia. J Geol Soc Lond 151: 83–90

Williams IS, Claesson S (1987) Isotopic evidence for the Precambrian provenance and Caledonian metamorphism of high grade paragneisses from the Seve Nappes, Scandinavian Caledonides. Contrib Mineral Petrol 97: 205–217

Willner AP, Rötzler K, Maresch W (1997) Pressure–temperature and fluid evolution of quartzo-feldspathic metamorphic rocks with a relic high-pressure, granulite-facies history from the Central Erzgebirge (Saxony, Germany). J. Petrol 38: 307–336

Zoubek V (1974) Remarques sur le Précambrien des zones mobiles de l'Europe Centrale et Occidentale. In: Zoubek V (ed) Précambrien des zones mobiles de l'Europe, Conf PICG, Liblice, Academia Prague, pp 33–62